Carbon atom condensation on NH_3-H_2O ices. An Alternative Pathway to Interstellar Methanimine and Methylamine

Germán Molpeceres,*,†,‖ Masashi Tsuge,‡ Kenji Furuya,¶ Naoki Watanabe,‡ David San Andrés,§ Víctor M. Rivilla,§ Laura Colzi,§ and Yuri Aikawa†

†*Department of Astronomy, Graduate School of Science, The University of Tokyo, Tokyo 113 0033, Japan*
‡*Institute of Low Temperature Science,Hokkaido University, Sapporo, Hokkaido 060-0819, Japan*
¶*National Astronomical Observatory of Japan, 181-8588, Tokyo, Japan*
§*Centro de Astrobiología (CAB), INTA-CSIC, Torrejón de Ardoz, 28850, Madrid, Spain*
‖*Grupo de Astrofísica Molecular, Instituto de Física Fundamental (IFF-CSIC), C/ Serrano 121, 28006 Madrid, Spain*

E-mail: molpeceres@astron.s.u-tokyo.ac.jp

Abstract

The recent discovery of the nature and behavior of carbon atoms interacting with interstellar ices has prompted a number of investigations on the chemistry initiated by carbon accretion on icy interstellar dust. In this work, we expand the range of processes promoted by carbon accretion to the chemistry initiated by the interaction of this atom with ammonia (NH_3) using quantum chemical calculations. We found that carbon addition to the ammonia molecule forms a rather stable radical, CNH_3, that is easily hydrogenated. The complete hydrogenation network is later studied. Our calculations reveal that, while conversion to simpler molecules like HCN and HNC is indeed a possible outcome promoted by H-abstraction reactions, methylamine is also easily formed (CH_3NH_2). In fact, the stability of methylamine against hydrogen abstraction, makes this molecule the preferred product of the reaction network. Our results serve as a stepping stone towards the accurate modeling of C-addition reactions in realistic astrochemical kinetic models.

1 Introduction

In the broad definition of interstellar complex organic molecules (COMs), we include all molecules with six or more atoms, of which at least one of them is a carbon atom.[1] Given the conditions found in molecular clouds, cold regions of the interstellar medium (ISM) with temperatures as low as 10 K and a low gas density, e.g. 1×10^4 cm^{-3}, the formation of COMs takes place under certain constraints. The formation of COMs may occur in the gas and on top of ice-covered dust grains. Generally speaking, we can separate the formation of COMs on dust grains occurring at low temperatures (10 K), dominated by hydrogenation, for example of solid CO,[2,3] and reactions that take place through diffusion of heavier radicals once the temperature starts to rise after the formation of a protostar (T$>$ 30 K).[4,5] In recent years, several additions to the hydrogenation of CO for the formation of COMs have appeared. For example, COMs synthesis through gas phase reactions,[6–10] non-thermal reactions on ice,[5,11] the emergence of kinetic barriers on water-rich ice surfaces,[12,13] or the topic under investigation in

this article, condensation of atomic carbon ((^{3}P)-C, abbreviated C) on interstellar ices.[14–20]

A long-standing assumption for the field of astrochemistry is that atoms (C, N, O), or small molecules (CO, N_2, C_2H) physisorb on ice surfaces, i.e., interact weakly with the surface.[21] This assumption has been found in recent years not to be generally true, with certain species being able to chemisorb and strongly interact with the surface.[15,19,22–27] Exploring the range of chemical processes derived from ice surfaces is a worthwhile effort to discover previously ignored chemical routes to COMs.

The carbon atom has proven to be an excellent promoter of chemistry. Several works found that C chemisorbs in amorphous solid water (ASW),[15,24,25] the most abundant ice phase in the ISM, following an Eley-Rideal mechanism.[28] The resulting C-H_2O complex from the chemisorption is better described as $^3COH_2$, a very reactive chemical species that can spontaneously evolve to H_2CO, as evinced by quantum chemical calculations and experiments.[15,20] Alternatively, C can also adsorb on physisorption sites, being able to diffuse until trapped in chemisorption sites, or react with other preadsorbed molecules, at around 22 K under ISM conditions.[20] Another abundant ice species with whom C is able to chemisorb and react is carbon monoxide, CO. Upon accretion, C chemically converts to CCO, a transient species easily hydrogenated to ketene H_2CCO and beyond under ISM conditions.[17,19] In this study we considered the interaction of C with ammonia (NH_3), another molecule that is abundant in interstellar ice. Krasnokutski et al.[18] performed co-deposition experiments of NH_3:CO:C, observing the formation of aminoketene (NH_2HCCO), and its polymerization. Using gas-phase calculations, Krasnokutski et al.[18], reported the formation of the CNH_3 adduct without a barrier, which is also supported by other works.[29,30] The evolution of the CNH_3 adduct in the codeposition experiments of Krasnokutski et al.[18] requires sufficient residence times on the surface to overcome the kinetic barriers proposed by these authors or another alternative mechanism conducive to NH_2HCCO. Furthermore, due to the lack of a H_2O matrix in Krasnokutski et al.[18], the resilience of CNH_3 in ASW has not yet been determined.

Another important implication of the resilience of CNH_3 radicals concerns their chemical conversion pathways. At 10 K, very few chemical species can diffuse on interstellar dust grains, for example, H atoms, He atoms, and H_2 molecules. It is not clear whether other species, such as CO, N or O, can diffuse at 10 K, although if they could, they should diffuse slowly.[31–34] In addition to fast diffusion, both H atoms and H_2 molecules can penetrate potential energy barriers due to quantum tunneling. Because H_2 is a stable closed-shell molecule, its related chemistry is restricted to just a few, but very important reactions.[35–37] H atoms, however, are very reactive and are the most important reagent on the surface of dust grains. The reason for this assertion is not only based on quantum chemical arguments, like the above-mentioned quantum tunneling effect, but also on astrochemical arguments. Hydrogen atoms are very abundant in molecular clouds owing to an efficient destruction of H_2 molecules by cosmic rays. Abundances are typically $\sim 2\times10^{-4}$ with respect to H_2 for canonical cosmic ray ionization rates in molecular clouds.[38] Hydrogen atoms participate in the hydrogenation reactions responsible for an increase in chemical complexity through hydrogen addition reactions,[2,39,40] but also in the reduction of chemical complexity through H-abstraction reactions.[41–43] While the cited studies are only a small portion of the plethora of studies on the hydrogenation of ISM molecules, a quick look into the literature reveals a prevalence of H-addition studies, because they are more easily validated by experiments.

In this work, we construct the complete reaction network for the reactivity of CNH_3 with H atoms. We study hydrogen addition and hydrogen abstraction reactions in an effort to determine whether the evolution of CNH_3 leads to the formation of COMs, most notably methylamine (CH_3NH_2) or, if, in contrast, H-abstraction reactions can also produce highly unsaturated molecules, such as HCN or HNC. We achieve our goal by performing quantum chemical calculations of the reactions in the reaction network on a $(H_2O)_{14}$ cluster to which we add a single NH_3 molecule upon which we study the adsorption of a C atom. A proportion of 1:14 is chosen to mimic the ratio found in the ice observations of molecular clouds.[44]

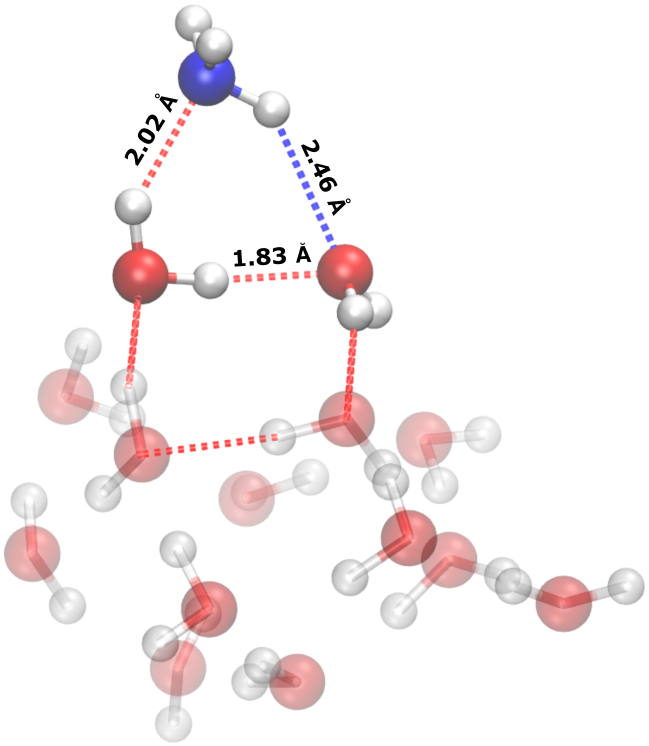

Figure 1: Optimized geometry for the $(H_2O)_{14}-NH_3$ cluster on which C adsorption and the subsequent hydrogenation reactions are studied. The dotted lines represent the H-bond network where proton transfer reactions are sampled. Red dots indicate the interactions a H-donor and blue dots indicate those where water is a H-acceptor. Solid molecules are used for the NH_3 and its direct H_2O neighbors. The code of colours employed throughout the article is: Red: Oxygen; Blue: Nitrogen; White: Hydrogen.

The structure of the article is as follows. In Section 2 we present the quantum chemical formalism for the study of the reactions, along with the caveats of treating such an extensive reaction network under a unified formalism. In Section 3 we study the reaction network. First, we focus on the study of the adsorption of C on NH_3. Secondly, we study in detail the ca. 40 reactions included in the reaction network. In Section 4 we discuss the implications on our findings in an astrochemical context, as well as compare with further results in the literature. We conclude with a brief summary of our results in Section 5.

2 Methods

The $(H_2O)_{14}$ cluster used for the ice structural model is taken from Molpeceres et al.[15]. After optimizing the cluster, we placed a NH_3 molecule on top of it. In particular, the physisorption arrangement that we selected involves the interaction of a dangling -OH bond that forms an H bond with the NH_3 molecule, and the -H donor interaction between the NH moiety of NH_3 and a contiguous H_2O molecule (see dashed red and blue lines in Figure 1). The donor acceptor motiff that we use is chosen to mimic the characteristic arrangement found for NH_3 on H_2O at the most likely binding sites, according to Tinacci et al.[45]. This is visually confirmed by the bond distances found for the adsorption of NH_3 in our cluster (Figure 1) and the ones found for average and deep binding sites in Tinacci et al.[45] (See their Figure 9). Moreover, the binding energy of NH_3 is $\sim$ 20 kJ mol^{-1} that is close to the most likely value found in the Maxwell-Boltzmann fit (μ=17.8 kJ mol^{-1} Figure 8 of Tinacci et al.[45]) of the binding energy distribution for the NH_3-H_2O system. In this arrangement, we also find a complementary four-center water H-bond network (four lowest dashed red lines in Figure 1), where we later test proton transfer reactions. After optimization of the $(H_2O)_{14}-NH_3$ cluster, we place a C atom forming an adduct with the NH_3 molecule, and begin to study all possible H addition and H-abstraction reactions following a common scheme. This scheme includes a potential energy surface (PES) scan, transition state search, and optimization of reactant and product from the end points of the potential energy scan, refining the geometries in the case the latter protocol reveals not to be a global minimum in the PES. For every stationary point on the PES that we obtain, we calculated its molecular Hessian. Reaction energies (ΔU^R) and activation energies ($\Delta U^\ddagger$) are obtained as energy differences, inclusive of zero-point vibrational energy (ZPVE), of the product-reactant and the transition state-reactant, respectively. Every reaction is studied in the most stable spin multiplicity of the products, which is singlet for most of the closed-shell molecules, doublet for the radicals, or triplet in the case of CNH_3 and H_3CN. The spin multiplicity of all reactants and products in this work is indicated in the detailed discussion

of every reaction.

Finally, to compare with the results on the ice, we repeated our study without the ice cluster to report the energetics of the gas-phase reactions along with the ones in the ice. It is important to note that the products of gas-phase reactions in this work do not directly translate into the products of these reactions at the low pressures of the ISM, especially for H-addition reactions. The notation 'Gas Phase" is used to reflect the fact that a water cluster was not employed in the study. The only difference in the protocol used in the gas phase study is that for barrierless reactions in the gas phase, the energetic parameters are computed from the bimolecular system (e.g. reactant + H) rather than the preadsorbed H and reactant on the ice cluster.

Compared to Molpeceres et al.[15], for the DFT method in this work we increased the basis set and added the D3BJ dispersion correction term to the MPWB1K functional, i.e., the MPWB1K-D3BJ/ma-def2-TZVP method.[46–51] The parameters for the D3BJ dispersion correction in that functional are taken from Goerigk et al.[52] All DFT calculations use a large integration grid (`defgrid3` in ORCA 5.0.4[53,54]). The selection of this functional and basis set follows the recommendation found in our previous work for the C−H_2O system.[15] Electronic energies for open-shell singlets, as well as a couple of radical-radical reactions in the doublet channel are not refined further. However, for all the rest of reactions, we refined the electronic energies of the stationary points of the reaction using the DLPNO-CCSD(T)/jun-cc-pV(T+d)Z method using a `tightPNO` localization scheme.[55–57] The latter cases are referred as A e.g. systems treated with DLPNO-CCSD(T)/jun-cc-pV(T+d)Z//MPWB1K-D3BJ/ma-def2-TZVP[i] level and the former, B, e.g. systems treated at the MPWB1K-D3BJ/ma-def2-TZVP level. We indicate in the text and accompanying tables when results are reported at one level or the other. It is important to recall that although DFT is a better choice than single reference wavefunction theory methods to study open-shell singlet systems, caution is advised when interpreting the results, in particular for the prediction of reactions not involving radical-radical couplings (e.g. H-abstraction reactions in the open-shell singlet channel). For this reason, we also confirm that several key reactions labeled "barrierless" later in the text are indeed barrierless using multireference calculations. The results are shown in the Supplementary Information. All calculations use the ORCA code (v 5.0.4),[58–60] except for the multireference calculations shown in the Supplementary Information. Reactions involving a biradical system are investigated following a broken-symmetry formalism converging the high-spin state and using those orbitals to converge the low-spin state, using the `FlipSpin` directive in ORCA.

We constructed our reaction network model, which is meant to be used for the rate equations, i.e. without tracing the positions of species on the ice surfaces. Although more sophisticated methods, e.g. microscopic Monte Carlo (e.g. Cuppen et al.[61]), can consider site-dependent reactions, their computational cost is significantly higher than the rate equation method. This compromise implies three caveats in our reaction network. First, it is important to note that the activation energies and reaction energies in our calculations depend on the binding mode of the H_xC-NH_y molecule. Because our reaction network contains species that are formed from different reaction routes, the binding modes of some species vary depending on the reaction route under consideration. This implies that there must be some variability for the activation and the heat of reaction. Second, when several H-abstraction reactions were available at the same atomic center, we selected the least impeded one in the ice model. Third, one species in the reaction network presents trans-cis isomerism (HCNH). For this species, we have studied the chemistry of cis-HCNH, which, despite being the highest energy isomer, is the one that is formed from H-addition reactions, observed from intrinsic reaction coordinate calculations (IRC). We observed the same behavior in the hydrogenation of the OCS molecule yielding the cis-OCSH radical.[39] Accepting these approximations, we reduce the extensive computational cost associated with this work and simplify the reaction network for easier inclusion in astrochemical models. The main drawback associated with these

[i]The "1//2" notation is used to indicate that single point calculations at the 1 level are carried out on top of level 2 geometries.

shortcomings is that we lose statistical insight on the variability of activation energies and reaction and report a single value out of a distribution of possible values.[62]

3 Results

A summary of the reaction network investigated in this work is shown in Figure 2, and Tables 1 and 2. In the following subsection, we describe the analysis of the chemical reactions. An important note during the section is that we adopt a common notation on the molecules like H_xCNH_y with the exception of HCN and HNC. This was done to visually identify the differences in the coordination of both C and N in the involved molecules. All reactions include the spin multiplicity of the reactants to better track the chemical reactions under investigation.

3.1 Barrierless association of C + NH_3

Our first test focuses on determining whether the addition of ^{3}C on NH_3 is barrierless on H_2O ice, i.e. the reaction:

$$^3\mathrm{C} + {}^1\mathrm{NH_3} \longrightarrow {}^3\mathrm{CNH_3}\,. \qquad (1)$$

Recently, Krasnokutski et al.[18] and Agúndez et al.[30] demonstrated, using gas-phase calculations, that the insertion of C into a NH_3 molecule is barrierless. However, it is worth checking to see if the same behavior is expected on ices. In Figure 3 we show a scan of the elongation of the C-N coordinate in the pre-adsorbed ^{3}C$-$$NH_3$ adduct. It is important to note that due to the reactivity of the carbon atom with H_2O, the scan must be carried out fixing the cartesian positions of the nitrogen atom of NH_3, and the two nearest oxygen atoms of H_2O at the binding site. Otherwise, during relaxation of the different coordinates from the C–N coordinate, C would condense on neighboring H_2O molecules. The reaction of C with nearby water molecules is a consequence of the calculation setup that does not imply a preference for adsorption of C on H_2O rather than on NH_3. Because during the scan the C-N coordinate is fixed by a constraint, the optimizer explores other low-energy situations, being the formation of COH_2 one of them. Fixing the coordinates has an effect on the reaction energy ΔE_r.[ii] In Figure 3, the reaction energy is around -175 kJ mol^{-1}, but this value is lower than the real one, that is $\Delta \mathrm{U}^{R,1}_{\mathrm{Ice}}$ = -153.5 kJ mol^{-1} at the B level and ZPVE inclusive. In reality, if the NH_3 and neighbor H_2O molecules could relax, the adsorption asymptote would shift towards lower values, as a consequence of the formation of an ideal NH_3-2 H_2O binding configuration. Following the same reasoning, if chemisorption entrance barriers were present, they would be higher in the constrained scan than in the full relaxed scan. Therefore, we confirm that the addition of C to NH_3 on an ice is barrierless, which is the most important information extracted from Figure 3.

Gauging which substrate for the C insertion is more favorable on real mixed interstellar ices is a very complex task. Intuitively, from our knowledge on gas-phase reactions, the preference of adsorption should depend on electrostatic magnitudes like the (local) dipole moment on the surface, because a stronger dipole would result in a larger long-range interaction, resembling a "capture" event. Under these considerations, NH_3 and H_2O should not have a preferential reactivity, because their dipole moments are similar. However, there is a simpler way of determining which adsorption events is more likely for equivalent dipole moments. Eley-Rideal rate constants, such as the ones of these adsorptions, depend on the surface coverage like:

$$k^i_{ER} = \theta^i f_{acc} = \theta^i S_{\mathrm{T}} \nu n_{\mathrm{grain}} \pi r^2_{\mathrm{grain}} n_{\mathrm{g}},$$

where θ^i is the surface coverage of a molecule, f_{acc} is the frequency of accretion, S_{T} is the sticking coefficient, ν the average thermal velocity of the gas and r^2_{grain} and n_{g} the grain average radius and number density, respectively. Because all parameters other than θ^i are equal between ices, θ^i is the determining factor. In molecular clouds, θ^i is normally an order of magnitude larger for H_2O than for NH_3, making reaction 1 less effective than ^{3}C + ^{1}H_2O $\longrightarrow$ ^{3}COH_2 (but possibly more effective than ^{3}C + ^{1}CO $\longrightarrow$ ^{3}CCO, at least in

[ii] Note that the points along the scan are not ZPVE corrected, hence the ΔE_r notation.

Table 1: Summary of all reactions considered in this work (Continues in Table 2). BL means "barrierless".

Label	Reaction	Level	Structural Model	ΔU^R (kJ mol^{-1})	$\Delta U^{\ddagger}$ (kJ mol^{-1})
1	$^3C + {}^1NH_3 \longrightarrow {}^3CNH_3$	B	Ice	-153.5	BL
2	$^3CNH_3 \longrightarrow {}^3HCNH_2$	A	Ice	-141.9	50.3*
3	$^3CNH_3 + {}^2H \longrightarrow {}^2HCNH_3$	B	Ice	-363.9	BL
		B	Gas	-337.7	BL
4	$^3CNH_3 + {}^2H \longrightarrow {}^2CNH_2 + {}^1H_2$	B	Ice	-388.6	BL
		B	Gas	-405.4	BL
5	$^2HCNH_3 \longrightarrow {}^2H_2CNH_2$	A	Ice	-217.7	BL
6	$^2H_2CNH_2 + {}^2H \longrightarrow {}^1H_3CNH_2$	B	Ice	-385.5	BL
		B	Gas	-372.6	BL
7**	$^2H_2CNH_2 + {}^2H \longrightarrow {}^1HCNH_2 + {}^1H_2$	B	Ice	N/A	N/A
		B	Gas	-108.7	BL
8**	$^2H_2CNH_2 + {}^2H \longrightarrow {}^1H_2CNH + {}^1H_2$	B	Ice	N/A	N/A
		B	Gas	-252.4	BL
9	$^1H_3CNH_2 + {}^2H \longrightarrow {}^2H_2CNH_2 + {}^1H_2$	A	Ice	-37.6	37.3
		A	Gas	-48.7	34.2
10	$^1H_3CNH_2 + {}^2H \longrightarrow {}^2H_3CNH + {}^1H_2$	A	Ice	-21.4	44.8
		A	Gas	-24.4	39.5
11	$^2CNH_2 \longrightarrow {}^2HCNH$	A	Ice	-67.9	88.8
12	$^2CNH_2 + {}^2H \longrightarrow {}^1HCNH_2$	B	Ice	-312.7	BL
		B	Gas	-332.1	BL
13	$^2CNH_2 + {}^2H \longrightarrow {}^3CNH_3$	A	Ice	-43.9	66.4
		A	Gas	-23.8	74.2
14	$^2CNH_2 + {}^2H \longrightarrow {}^1HNC + {}^1H_2$	B	Ice	-368.7	BL
		B	Gas	-368.7	BL
15	$^1HNC + {}^2H \longrightarrow {}^2CNH_2$	A	Ice	-48.3	55.6
		A	Gas	-38.9	59.1
16	$^1HNC + {}^2H \longrightarrow {}^2HCNH$	A	Ice	-101.9	8.1
		A	Gas	-110.8	11.9
17	$^2HCNH + {}^2H \longrightarrow {}^1H_2CNH$	B	Ice	-417.1	BL
		B	Gas	-406.0	BL
18	$^2HCNH + {}^2H \longrightarrow {}^1HCNH_2$	B	Ice	-284.5	BL
		B	Gas	-261.6	BL
19	$^2HCNH + {}^2H \longrightarrow {}^1HNC + {}^1H_2$	B	Ice	-311.4	BL
		B	Gas	-298.3	BL
20	$^2HCNH + {}^2H \longrightarrow {}^1HCN + {}^1H_2$	B	Ice	-344.2	BL
		B	Gas	-350.6	BL
21	$^1H_2CNH + {}^2H \longrightarrow {}^2H_3CNH$	A	Ice	-127.7	15.1
		A	Gas	-127.9	15.8
22	$^1H_2CNH + {}^2H \longrightarrow {}^2H_2CNH_2$	A	Ice	-150.6	19.4
		A	Gas	-152.4	17.6
23	$^1H_2CNH + {}^2H \longrightarrow {}^2HCNH + {}^1H_2$	A	Ice	-14.5	45.0
		A	Gas	-15.6	46.4
24	$^1H_2CNH + {}^2H \longrightarrow {}^2H_2CN + {}^1H_2$	A	Ice	-62.9	23.8
		A	Gas	-73.2	19.5
25	$^1HCNH_2 \longrightarrow {}^1H_2CNH$	A	Ice	-122.7	22.7
26	$^1HCNH_2 + {}^2H \longrightarrow {}^2H_2CNH_2$	A	Ice	-268.8	BL
		A	Gas	-298.5	BL
27	$^1HCNH_2 + {}^2H \longrightarrow {}^2HCNH_3$	A	Ice	-55.5	101.9
		A	Gas	-26.9	73.8
28	$^1HCNH_2 + {}^2H \longrightarrow {}^2CNH_2 + {}^1H_2$	A	Ice	-109.3	3.5
		A	Gas	-91.1	5.8

(*) - Upper limit

(**) - There is evidence for these reactions to be non competitive with Reaction 6 (See section 3.2.2)

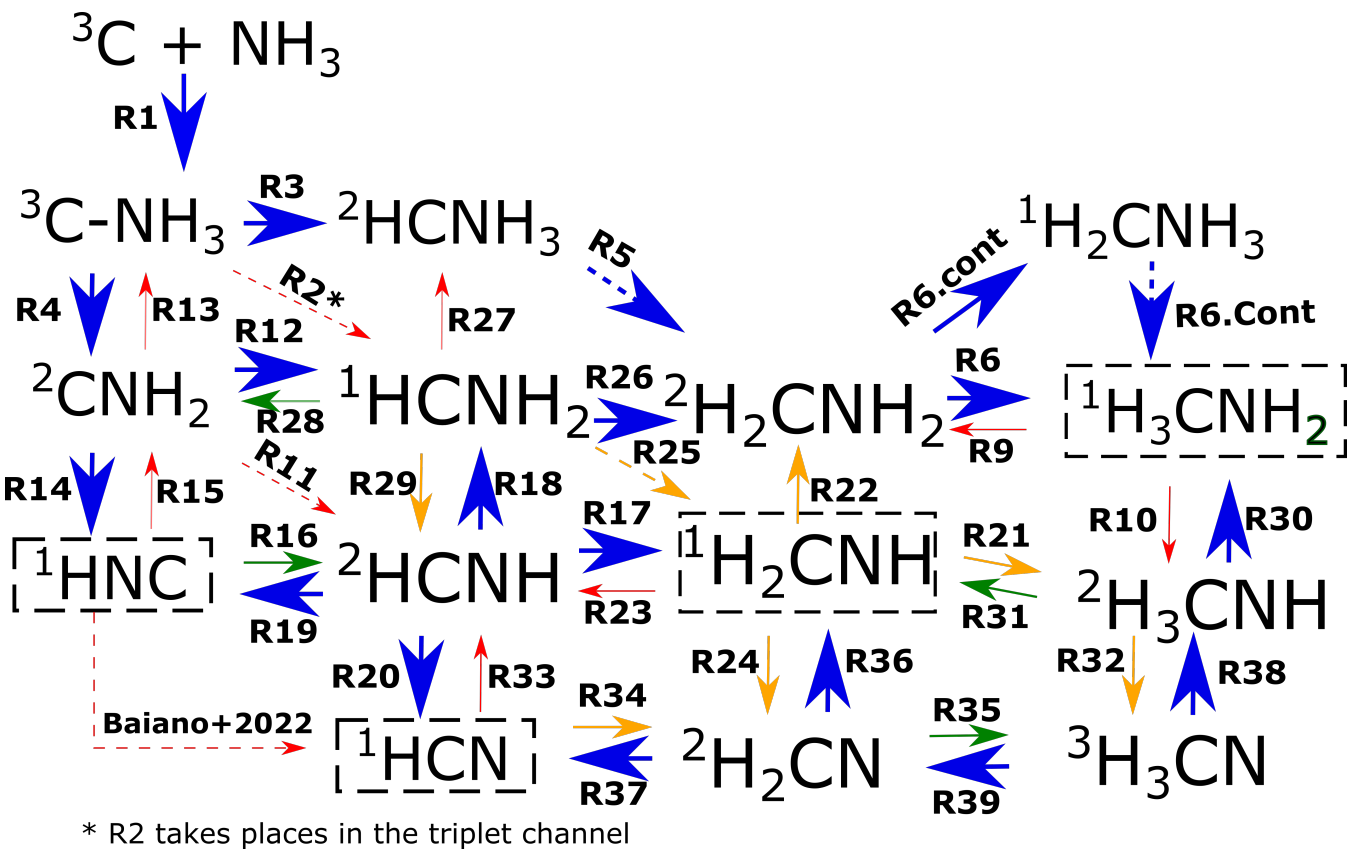

Figure 2: Reaction network investigated in this work showing our main findings. Dashed boxes on HNC, HCN, H_2CNH and H_3CNH_2 denote these molecules as the stable nodes in the reaction network. The colors of the arrows used in the reaction network have been selected according to $\Delta U^{\ddagger}$ obtained in the $(H_2O)_{14}$ cluster. Blue thick arrows denote barrierless reactions. Yellow and green arrows denote reaction with $10 < \Delta U^{\ddagger} < 30$ kJ mol $^{-1}$ and $\Delta U^{\ddagger} < 10$ kJ mol $^{-1}$. Red small arrows indicate reactions with high $\Delta U^{\ddagger}$ (> 30 kJ mol $^{-1}$). Solid lines are used for H-addition and H-abstraction reactions whereas dashed lines are used for proton transfer reactions. The HNC $\longrightarrow$ HCN isomerization is taken from Baiano et al.[63]. The legend RX above every reaction arrow corresponds to the numerical values shown in Tables 1 and 2. Note that 10 kJ mol^{-1} equals 1202 K.

young molecular clouds). However, we note that this does not disqualify the importance of the formation of CNH_3, because it could be a new formation path for N-bearing COMs, as discussed in Section 3.2.2.

It is also interesting to compare the adsorption energies (i.e. reaction energies) between the different adsorbates that have been recently studied in the literature. Such a comparison is held in Table 3. We observe a high variability between the reaction energies for the three species considered H_2O / CO /NH_3, with the highest reaction energy corresponding to CO. This is probably attributable to the formation of a formal double bond in the case of CCO, in comparison with the other two. More complex to explain is the difference between NH_3/H_2O and H_2O ice clusters, but in this case the differences are also subtler. We note that in order to carry a proper comparison, reaction 1 should be studied on pure NH_3 ice, and not in a diluted mixture such as the one of this work. It is important to note that the thermodynamic stability is not a good estimator of the larger viability of C condensation in any substrate and that preference for adsorption comes from different factors, such as surface coverage and attractive C-X potential (See above). Overall, we find that all adsorption energies forming these chemisorbates are very high when comparing with e.g. the barrier for diffusion. Hence all these species should remain immobile in molecular clouds.

Table 2: Continuation of Table 1. BL means "barrierless".

Label	Reaction	Level	Structural Model	ΔU^R (kJ mol^{-1})	$\Delta U^{\ddagger}$ (kJ mol^{-1})
29	$^1HCNH_2 + {}^2H \longrightarrow {}^2HCNH + {}^1H_2$	A	Ice	-171.2	22.7
		A	Gas	-163.2	29.4
30	$^2H_3CNH + {}^2H \longrightarrow {}^1H_3CNH_2$	B	Ice	-403.3	BL
		B	Gas	-400.3	BL
31	$^2H_3CNH + {}^2H \longrightarrow {}^1H_2CNH + {}^1H_2$	B	Ice	-288.2	1.8
		B	Gas	-281.3	1.3
32	$^2H_3CNH + {}^2H \longrightarrow {}^3H_3CN + {}^1H_2$	A	Ice	-76.3	12.9
		A	Gas	-85.8	8.8
33	$^1HCN + {}^2H \longrightarrow {}^2HCNH$	A	Ice	-43.0	37.3
		A	Gas	-52.1	41.3
34	$^1HCN + {}^2H \longrightarrow {}^2H_2CN$	A	Ice	-110.0	20.1
		A	Gas	-108.5	25.4
35	$^2H_2CN + {}^2H \longrightarrow {}^3H_3CN$	A	Ice	-140.6	9.0
		A	Gas	-142.7	11.1
36	$^2H_2CN + {}^2H \longrightarrow {}^1H_2CNH$	B	Ice	-357.5	BL
		B	Gas	-350.9	BL
37	$^2H_2CN + {}^2H \longrightarrow {}^1HCN + {}^1H_2$	B	Ice	-291.3	BL
		B	Gas	-296.2	BL
38	$^3H_3CN + {}^2H \longrightarrow {}^2H_3CNH$	B	Ice	-346.8	BL
		B	Gas	-335.7	BL
39	$^3H_3CN + {}^2H \longrightarrow {}^2H_2CN + {}^1H_2$	B	Ice	-269.9	BL
		B	Gas	-264.6	0.5

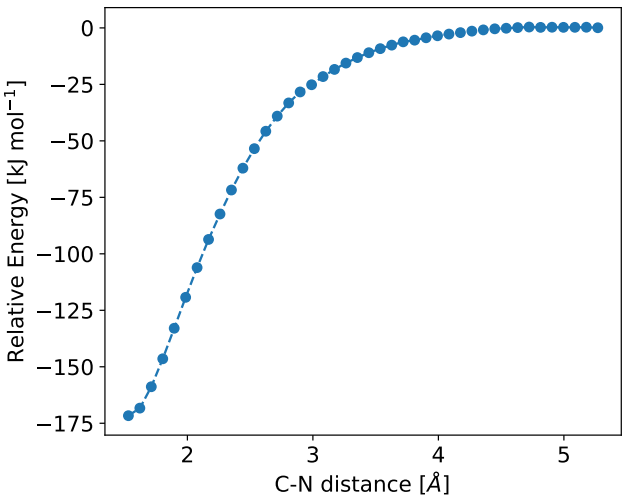

Figure 3: Potential energy scan for the C-N reaction coordinate in the $^3C + {}^1NH_3 \longrightarrow {}^3CNH_3$ reaction at the (B) level of theory. The points along the scan are not ZPE corrected.

3.2 Hydrogenation reactions

In this section we delve into the reaction of CNH_3 and its associated products with H atoms, due to the importance of this species as we presented in the introduction. We note that hydrogenation in this work refers to reactions with H, a nomenclature not distinguishing H-addition or H-abstraction reactions.

Table 3: Comparison between ΔU^R (in kJ mol^{-1}) for different C condensation reactions.

Ice Cluster	ΔU^R	References
Pure H_2O	96.0*/113.7**	[15] /[27]
Pure CO	207.5***	[64] /[19]
NH_3/H_2O	153.5	This work

*Average of a distribution of values (60–133 kJ mol^{-1})

**Average of three values (110.2–116.2 kJ mol^{-1})

***MRCI+Q gas phase values

3.2.1 Evolution of $^3CNH_3$

Establishing a parallelism with the chemisorption of C on H_2O that produces HCOH (and H_2CO) after adsorption on some binding sites, it is reasonable to think that $^3CNH_3$ may undergo a unimolecular conversion to $^3HCNH_2$. Another possible conversion pathway involves an initial decay to the singlet state ($^1CNH_3$) promoted by an intersystem crossing and subsequent evolution to $^1HCNH_2$ by a proton transfer.

We checked both outcomes at the (B) level of theory, finding that $^3CNH_3$ is stable in the triplet state and the singlet $^1CNH_3$ is 50.3 kJ mol^{-1}

higher in energy. Furthermore, we investigate whether the $-NH_3$ moiety can transfer a proton to a neighboring water molecule and evolve to $^3HCNH_2$ spontaneously through the following reaction on a water surface:

$$^3CNH_3 \longrightarrow {}^3HCNH_2, \qquad (2)$$

Finding the transition state for the reaction 2 was challenging and we needed to loose the convergence criteria on the optimization procedure. We finally converged to a structure shown in Figure 4 with a large transition frequency (approximately $650i$ cm^{-1}) corresponding to the reaction mode but also with two imaginary low-frequency modes not associated with the reaction mode. This structure has a high activation energy (at the A level of theory) of $\Delta U^{\ddagger,2}_{Ice}$ = 50.3 kJ mol^{-1} ($\Delta U^{R,2}_{Ice}$ = -141.9 kJ mol^{-1}), which given the subpar nature of the structure, we consider as an upper limit for the real activation energy. Because other proton transfer reactions studied in this work were found to be viable (see the next sections), we then determine that our activation energy for this reaction must be high enough to consider reaction 2 not important in astrophysical environments. We note that these proton transfer reactions depend on the local water arrangements[15,27,63] and that different barriers could be present at different binding sites. However, the value we obtained of the activation energy is much higher than the highest one found for $^3COH_2 \longrightarrow {}^3HCOH$ (around 11.5 kJ mol^{-1} as a maximum), which prompts us to consider $^3CNH_3$ as a more stable molecule on the surface. The chemical reason for this is probably found in the electronegativity of N with respect to O, which makes NH_2 polarize the C atom less, making it less prone to proton transfer.

As the unimolecular reactions have very high activation barrier, the most probable reaction for $^3CNH_3$ on ice surface is hydrogenation through the following reactions:

$$^3CNH_3 + {}^2H \longrightarrow {}^2HCNH_3 \qquad (3)$$
$$^3CNH_3 + {}^2H \longrightarrow {}^2CNH_2 + {}^1H_2 \qquad (4)$$

The first reaction (3) is a barrierless addition reaction that we studied in the double channel using

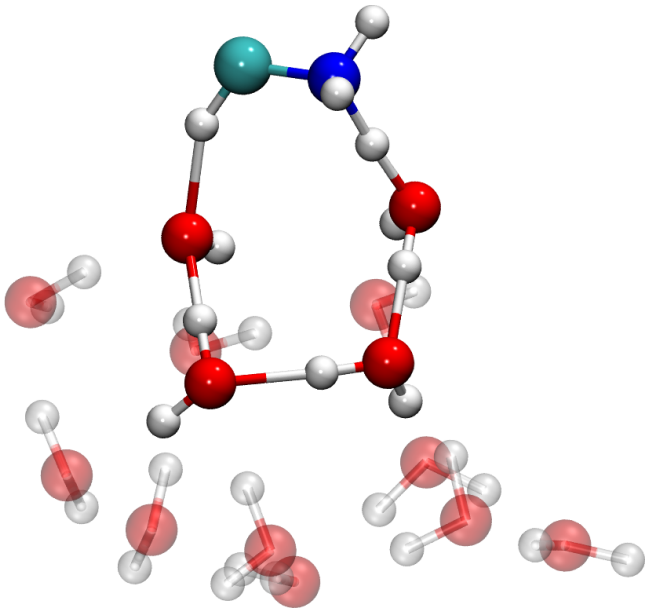

Figure 4: Geometry of the transition state corresponding to reaction 2. Color labels are equivalent to the ones in Figure 1 with the addition of Teal for the carbon atom.

the `FlipSpin` feature in ORCA. First, we converge the quartet state solution, and then we converge the doublet one from the previous orbitals. We found the reaction to be barrierless, with a reaction energy on ice of $\Delta U^{R,3}_{Ice}$ = -363.9 kJ mol^{-1} and in the gas of $\Delta U^{R,3}_{Gas}$ = -337.7 kJ mol^{-1} indicating a strong influence of the binding energy on the water ice of reactant and product. These results are at the B level of theory. The reaction studied without the water cluster is also barrierless.

The H-abstraction reaction 4, calculated using the same method and protocol as above, is also very exothermic $\Delta U^{R,4}_{Ice}$ = -388.6 kJ mol^{-1} ($\Delta U^{R,4}_{Gas}$ = -405.4 kJ mol^{-1}), although the difference between the surface and gas values is less pronounced. Interestingly, for both the reaction on ice and the reaction in the gas, we find tiny activation energies of < 2 kJ mol^{-1} that vanish upon inclusion of ZPVE, making the reaction effectively barrierless.

Therefore, the hydrogenation reactions 3 and 4 are barrierless, fast reactions that readily convert the $^3CNH_3$ adduct at low-temperature H-rich environments. Because unimolecular reactions from CNH_3 are unlikely due to the high barriers, these first hydrogenation reactions (Reactions 3 and 4) lock the hydrogenation route towards the forma-

tion of small isocyanic (HNC) and cyanic (HCN) acids, or toward the formation of more hydrogenated products like methylamine CH_3NH_2 or methanimine CH_2NH. The reactions leading to one or the other outcome are explicitly considered in the following sections.

3.2.2 Formation of H_3CNH_2 from CNH_3

Once $^3CNH_3$ is formed and hydrogenated, the nodes in the reaction network can evolve toward the formation of H_3CNH_2 (methylamine, commonly writen as CH_3NH_2). The simplest pathway connecting hydrogenated $^3CNH_3$ and H_3CNH_2:

$$^2HCNH_3 \longrightarrow {}^2H_2CNH_2, \qquad (5)$$

through a sequential proton transfer reaction. More details about this reaction are given in the supplementary information. Reaction 5 it is then followed by hydrogenation to CH_3NH_2 *via*:

$$^2H_2CNH_2 + {}^2H \longrightarrow {}^1H_3CNH_2 \qquad (6)$$

In addition to the above reaction, another possible reaction is the H-addition at the $-NH_2$ moiety that generates a $-NH_3$ group, e.g. δ^+ on the nitrogen atom, that quickly isomerizes to the more stable H_3CNH_2 isomer. We carried out PES scans for the $^2H_2CNH_2 + {}^2H \longrightarrow {}^1H_2CNH_3$ reaction at the B level observing a direct conversion to H_3CNH_2. Hence, $H_2CNH_2 + H \longrightarrow H_2CNH_3$ is equivalent to reaction 6.

Reaction 5 presents a submerged barrier $\Delta U^{\ddagger,5}_{Ice}$ = -2.3 kJ mol^{-1} upon inclusion of ZPVE, and a reaction energy of $\Delta U^{R,5}_{Ice}$ = -217.7 kJ mol^{-1}. Because the reaction occurs in the doublet channel, the above results are at the A level of theory. Reaction 5 occurs before $HCNH_3$ undergoes additional hydrogenation. Although different binding sites for $HCNH_3$ can inhibit direct isomerization through reaction 5, the absence of a barrier for proton transfer strongly suggests a very reactive nature. In light of these results, we do not expect $HCNH_3$ a dectectable species in the ISM.

Concerning reaction 6, the addition to C produces H_3CNH_2. In both the gas phase and the ice, we found that the reaction 6 was barrierless, with reaction energies of $\Delta U^{R,6}_{Ice}$ = -385.5 kJ mol^{-1} and $\Delta U^{R,6}_{Gas}$ = -372.6 kJ mol^{-1} at the B level of theory because the reaction takes place in the open-shell singlet channel.

These paths do not compete with hydrogen abstraction reactions, because back proton transfer reactions are endothermic and the following reactions:

$$^2H_2CNH_2 + {}^2H \longrightarrow {}^1HCNH_2 + {}^1H_2 \qquad (7)$$
$$^2H_2CNH_2 + {}^2H \longrightarrow {}^1H_2CNH + {}^1H_2 \qquad (8)$$

are found to be non-viable on the ice cluster. These reactions are very complex to study on the ice model from a technical point of view, due to competition with reaction 6, which drives in many cases the geometry optimizer to the addition product (H_3CNH_2). This leads us to conclude that reactions 7 and 8 are not competitive against reaction 6 even though in the gas phase these reactions are barrierless (see below). The reason for our conclusion is that the geometry optimizer behavior indicates an easier reaction channel in reaction 6, at least in a water environment. From the perspective of the astrochemical models, the picture left by these reactions suggests that only the reaction 6 should be included in models with a branching ratio of 1.0 in the subset of reactions 6–8. However, our conclusion requires experimental validation or, in its absence, a theoretical study involving larger sampling at different binding sites, especially when looking at the reaction in the gas reported below.

It is worth noting that, in the gas phase, Joshi and Lee [65] found that the reactions 7 and 8 are barrierless. Our gas-phase calculations show the same result, confirmed by Nudget Elastic Band (NEB) calculations [66] using an open-shell singlet reference with a reaction energy of $\Delta U^{R,7}_{Gas}$ = -108.7 kJ mol^{-1} and $\Delta U^{R,8}_{Gas}$ = -252.4 kJ mol^{-1}. We note, however, that our own MRCI+Q calculations for reaction 7 (Supplementary Information) show an activation barrier while Reaction 8 is still found barrierless.

3.2.3 Destruction of CH_3NH_2

The fully saturated methylamine molecule can still be processed by H atoms back to the precursor radicals. The abstraction reactions that we have considered are:

$$^1H_3CNH_2 + {}^2H \longrightarrow {}^2H_2CNH_2 + {}^1H_2 \quad (9)$$
$$^1H_3CNH_2 + {}^2H \longrightarrow {}^2H_3CNH + {}^1H_2 \quad (10)$$

Both systems can be treated with the (A) level of theory. The reaction 9 has an activation energy $\Delta U^{\ddagger,9}_{Ice}$ = 37.3 kJ mol^{-1} whereas reaction 10 presents an activation energy of $\Delta U^{\ddagger,10}_{Ice}$ = 44.8 kJ mol^{-1}. The reaction energies were found to be $\Delta U^{R,9}_{Ice}$ = -37.6 kJ mol^{-1} and $\Delta U^{R,10}_{Ice}$ = -21.4 kJ mol^{-1} for reactions 9 and 10, respectively.

The energetic parameters for reaction 9 in the gas phase are $\Delta U^{\ddagger,9}_{Gas}$ = 34.2 kJ mol^{-1} and $\Delta U^{R,9}_{Gas}$ = -48.7 kJ mol^{-1} while for reaction 10 they are $\Delta U^{\ddagger,10}_{Gas}$ = 39.5 kJ mol^{-1}, $\Delta U^{R,10}_{Gas}$ = -24.4 kJ mol^{-1}. Therefore, we found that the activation energy gap between reaction 9 and 10 increases on ice, further confirming that reaction 9 is the preferred abstraction channel in H_3CNH_2. We note excellent agreement with the preceding work of Joshi and Lee[65] and Kerkeni and Clary[67], which reports activation energies of 33.4/36.8 and 39.7/39.2 kJ mol^{-1} for reactions 9/10 in the gas phase. The activation energies that we report for H_3CNH_2 are too high to represent an effective reaction path. However, we note that both Joshi and Lee[65] experiments in para-hydrogen and Oba et al.[68] in a methylamine matrix found plausible hydrogen abstraction, so we continue to recommend including reaction 9 and 10 in astrochemical reaction networks.

3.2.4 Formation of HNC

In section 3.2.2 we showed the least impeded channel from CNH_3 to H_3CNH_2, but as we showed in Section 3.2.1, $^3CNH_3$ can also experience H-abstraction reactions (Reaction 4), forming CNH_2 (Aminomethylidyne). Similarly, CNH_2 can react in our reaction network in four different ways:

$$^2CNH_2 \longrightarrow {}^2HCNH \quad (11)$$
$$^2CNH_2 + {}^2H \longrightarrow {}^1HCNH_2 \quad (12)$$
$$^2CNH_2 + {}^2H \longrightarrow {}^3CNH_3 \quad (13)$$
$$^2CNH_2 + {}^2H \longrightarrow {}^1HNC + {}^1H_2. \quad (14)$$

Reaction 11 is a proton transfer reaction for the spontaneous evolution of CNH_2. We sought the transition state of the reaction using NEB calculations, as in the previous examples. These NEB calculations were very difficult to converge on and required an increase in optimization tolerance. When a transition state was finally found, we refined it with a TS search using the dimer method[69] and standard convergence criteria. As in the case of CNH_3 described above, after this procedure we managed to converge on a stationary point in the PES. However, this transition state shows an additional spurious imaginary frequency of low magnitude ($12i$ cm^{-1}) that, after inspection, corresponds to a motion outside of the reaction center, and therefore we consider the TS that we found not ideal, but sufficiently reliable. Reaction 11 is exothermic ($\Delta U^{R,11}_{Ice}$ = -67.9 kJ mol^{-1}) but shows a rather high activation energy, $\Delta U^{\ddagger,11}_{Ice}$ = 88.8 kJ mol^{-1}. Therefore, we determine that the reaction 11 should not contribute significantly to the reaction network investigated in this work. We note that the product of the reaction 11 is trans-HCNH, but given the null viability of this reaction in the ISM, the choice of cis-HCNH isomer in further reactions in this work remains valid.

Reactions 12 and 14 are studied at the B level of theory because they are radical couplings in the singlet channel. On the other hand reaction 13 is studied at the more accurate A level because it takes place in a triplet PES. Reaction 12 is barrierless in both ice and gas, with a reaction energy of $\Delta U^{R,12}_{Ice}$ = -312.7 kJ mol^{-1} ($\Delta U^{R,12}_{Gas}$ = -332.1 kJ mol^{-1}). In contrast, the reaction 13 back to the CNH_3 shows an activation energy of $\Delta U^{\ddagger,13}_{Ice}$ = 66.4 kJ mol^{-1} ($\Delta U^{\ddagger,13}_{Gas}$ = 74.2 kJ mol^{-1}) and is barely exothermic $\Delta U^{R,13}_{Ice}$ = -43.9 kJ mol^{-1} ($\Delta U^{R,13}_{Gas}$ = -23.8 kJ mol^{-1}). Thus, return to CNH_3 from CNH_2 is inhibited, which combined with the reaction $^3CNH_3 + {}^2H \longrightarrow {}^2HCNH_3$ (Reaction 3) shows that the destruction *via* hydrogenation of CNH_3 is irreversible.

Finally, the H-abstraction reaction 14 is also barrierless with reaction energies $\Delta U^{R,14}_{Ice}$ = -368.7 kJ mol^{-1} ($\Delta U^{R,14}_{Gas}$ = -368.7 kJ mol^{-1}). This reaction forms HNC, one of the endpoints of the reaction network (Figure 2).

The CNH_2 radical is very reactive although it is detected in the ISM,[70,71] as shown by the barrierless nature of the reactions that we studied. However, we found that the return to CNH_3 through

the reaction 13 is not efficient, which indicates that evolution to the closed shell end points of the reaction network is the expected behavior after C chemisorption on NH_3.

3.2.5 HNC hydrogenation: Conversion to HCN and hydrogenation pathways to H_3CNH_2

After HNC is formed, several possibilities for reactions appear. The most immediate one involves direct isomerization to HCN through a proton transfer reaction, HNC $\longrightarrow$ HCN (in reality an equilibrium), Baiano et al.[63] investigated this reaction finding very low reaction rate constants at 10 K, not competitive with hydrogenation, considering an accretion rate of H under ISM conditions of one atom per day.[72] Morever, the $HNC + H \longrightarrow CN + H_2$ reaction is endothermic. Thus HNC can further react through the following reactions:

$$^1HNC + {}^2H \longrightarrow {}^2CNH_2 \quad (15)$$
$$^1HNC + {}^2H \longrightarrow {}^2HCNH. \quad (16)$$

Beginning with reaction 15, the reaction has a barrier of $\Delta U^{\ddagger,15}_{Ice}$ = 55.6 kJ mol^{-1} ($\Delta U^{\ddagger,15}_{Gas}$ = 59.1 kJ mol^{-1}) and $\Delta U^{R,15}_{Ice}$ = -48.3 kJ mol^{-1} ($\Delta U^{R,15}_{Gas}$ = -38.9 kJ mol^{-1}). This is due to the lower thermodynamic stability of the CNH_2 radical *versus* H_2CN. However, resistance to reaction 15 is counteracted by reaction 16, which presents activation energies of only $\Delta U^{\ddagger,16}_{Ice}$ = 8.1 kJ mol^{-1} ($\Delta U^{\ddagger,16}_{Gas}$ 11.9 kJ mol^{-1}), that is, very small activation energies that can be easily surmounted by quantum tunneling. The reaction energy of reaction 16 is $\Delta U^{R,16}_{Ice}$ = -101.9 kJ mol^{-1} ($\Delta U^{R,16}_{Gas}$ = -110.8 kJ mol^{-1}). Therefore, hydrogen addition to HNC must proceed through reaction 16

The two resulting radicals of reactions 15 and 16, can continue reacting. We turn our focus initially to cis-HCNH, that, as a central species of the reaction network, can evolve in four different directions:

$$^2HCNH + {}^2H \longrightarrow {}^1H_2CNH \quad (17)$$
$$^2HCNH + {}^2H \longrightarrow {}^1HCNH_2 \quad (18)$$
$$^2HCNH + {}^2H \longrightarrow {}^1HNC + {}^1H_2 \quad (19)$$
$$^2HCNH + {}^2H \longrightarrow {}^1HCN + {}^1H_2. \quad (20)$$

Proton transfer reactions, $^2HCNH \longrightarrow {}^2CNH_2$ and $^2HCNH \longrightarrow {}^2H_2CN$ cannot proceed in the binding sites that we encountered. Moreover, $^2HCNH \longrightarrow {}^2CNH_2$ is endothermic. Regarding hydrogenation reactions, 17 and 18 were found to be barrierless both in ice and gas. The reaction energies show two very exothermic reactions with $\Delta U^{R,17}_{Ice}$ = -417.1 kJ mol^{-1} ($\Delta U^{R,17}_{Gas}$ = -406.0 kJ mol^{-1}) for reaction 17 and $\Delta U^{R,18}_{Ice}$ = -284.5 kJ mol^{-1} ($\Delta U^{R,18}_{Gas}$ = -261.6 kJ mol^{-1}) for reaction 18.

The abstraction reactions 19 and 20 are also found to be barrierless with reaction energies of $\Delta U^{R,19}_{Ice}$ = -311.4 kJ mol^{-1} ($\Delta U^{R,19}_{Gas}$ = -298.3 kJ mol^{-1}) and $\Delta U^{R,20}_{Ice}$ = -344.2 kJ mol^{-1} ($\Delta U^{R,20}_{Gas}$ = -350.6 kJ mol^{-1}) for reactions 19 and 20, respectively. Interestingly, reaction 19 is less exothermic in the gas-phase, whereas reaction 20 is more exothermic in the gas-phase. This hints at a higher relative affinity of HNC with the surface compared to HCN. Nevertheless, HCN is still the favored isomer. It is worth mentioning that we found a transition state in the electronic energies in reaction 20, and in the ice. Barriers that are absent in the gas phase but present in the ice are normally attributed to the break of interactions between substrates with the surface, i.e. hydrogen bonds, restricted rotations, and have been carefully characterized lately.[13] These barriers are less common in reactions with H, due to weak interactions of H with the surface. Although the behavior of the reaction 20 is indeed interesting from a chemical point of view, for the purpose of this work, we find that the barrier submerges upon inclusion of ZPVE, rendering the reaction barrierless. The combination of reactions 16 and 20 results in the facile H mediated isomerization of HNC to HCN.

Because cis-HCNH has several barrierless branches when reacting with hydrogen there are other possibilities than the formation of HCN and HNC. One is conversion to the more complex species, H_2CNH (methanimine), the simplest

imine and one of the first precursors of nitrogen-bearing COMs that were assumed to be present in the ISM.[73] The other is hydrogenation at the NH moiety to form the higher-energy isomer of H_2CNH, aminomethylene ($HCNH_2$), that has recently been spectroscopically characterized.[74] Beginning with the chemistry of the former, we find the following reactions:

$$^1H_2CNH + {}^2H \longrightarrow {}^2H_3CNH \quad (21)$$
$$^1H_2CNH + {}^2H \longrightarrow {}^2H_2CNH_2 \quad (22)$$
$$^1H_2CNH + {}^2H \longrightarrow {}^2HCNH + {}^1H_2 \quad (23)$$
$$^1H_2CNH + {}^2H \longrightarrow {}^2H_2CN + {}^1H_2. \quad (24)$$

Starting our analysis of the reactions with the additions, reaction 21 has an activation energy of $\Delta U^{\ddagger,21}_{Ice}$ = 15.1 kJ mol^{-1} ($\Delta U^{\ddagger,21}_{Gas}$ = 15.8 kJ mol^{-1}) and an exothermicity of $\Delta U^{R,21}_{Ice}$ = -127.7 kJ mol^{-1} ($\Delta U^{R,21}_{Gas}$ = -127.9 kJ mol^{-1}). Reaction 22 shows slightly higher activation energies $\Delta U^{\ddagger,22}_{Ice}$ = 19.4 kJ mol^{-1} ($\Delta U^{\ddagger,22}_{Gas}$ = 17.6 kJ mol^{-1}) and similar reaction energies, i.e. $\Delta U^{R,22}_{Ice}$ = -150.6 kJ mol^{-1} ($\Delta U^{R,22}_{Gas}$ = -152.4 kJ mol^{-1}). The reaction 22 was studied in the gas phase by Joshi and Lee[65] finding an activation energy of 12.7 kJ mol^{-1}, slightly lower than our values reported above.

The H abstractions (reactions 23 and 24) present higher activation energies. In particular, reaction 23 has an activation energy of $\Delta U^{\ddagger,23}_{Ice}$ = 45.0 kJ mol^{-1} ($\Delta U^{\ddagger,23}_{Gas}$ = 46.4 kJ mol^{-1}) and a reaction energy of $\Delta U^{R,23}_{Ice}$ = -14.5 kJ mol^{-1} ($\Delta U^{R,23}_{Gas}$ = -15.6 kJ mol^{-1}), so the reaction has a very high activation energy and is barely exothermic. In contrast, the activation energy for reaction 24 is $\Delta U^{\ddagger,24}_{Ice}$ = 23.8 kJ mol^{-1} ($\Delta U^{\ddagger,24}_{Gas}$ = 19.5 kJ mol^{-1}) and $\Delta U^{R,24}_{Ice}$ = -62.9 kJ mol^{-1} ($\Delta U^{R,24}_{Gas}$ = -73.2 kJ mol^{-1}). Although the hydrogenation of H_2CN is later shown to be easier than that of H_2CNH (Section 3.2.6), the reaction 24 may permit some degree of interconversion and evolution to other nodes of the reaction network. In conclusion, reaction 24 might be plausible, whereas the high activation energy of reaction 23 makes it unlikely in astrophysical environments.

Returning to the high energy isomer $HCNH_2$, its reactivity with H is as follows:

$$^1HCNH_2 \longrightarrow {}^1H_2CNH \quad (25)$$
$$^1HCNH_2 + {}^2H \longrightarrow {}^2H_2CNH_2 \quad (26)$$
$$^1HCNH_2 + {}^2H \longrightarrow {}^2HCNH_3 \quad (27)$$
$$^1HCNH_2 + {}^2H \longrightarrow {}^2CNH_2 + H_2 \quad (28)$$
$$^1HCNH_2 + {}^2H \longrightarrow {}^2HCNH + H_2. \quad (29)$$

The investigation of reaction 25 was carried out using a combination of NEB calculations and TS refinement using the dimer method.[69] We use DL-FIND/CHEMSHELL[53,54] for this task. The isomerization *via* the proton transfer presents a barrier at the A level of $\Delta U^{\ddagger,25}_{Ice}$ = 22.7 kJ mol^{-1} and is exothermic with a reaction energy of $\Delta U^{R,25}_{Ice}$ = -122.7 kJ mol^{-1}. This reaction is only possible on ice. Interestingly, the reaction shows an abnormally low transition frequency of $\sim 70i$ cm^{-1}. An inspection of the transition mode confirms that it is associated with the formation of the product. The activation energy for this reaction is in reasonable agreement with that found in Ferrero et al.[27], of 14 kJ mol^{-1}. Because proton transfer reactions depend sensitively on the local topology of the H-bond network, both our values and Ferrero et al.[27] are likely valid and represent different points of a distribution of values. Although 22.7 kJ mol^{-1} is not a very high barrier, dedicated calculations that include nuclear quantum effects are desirable to check whether the reaction is fast enough to consider $HCNH_2$ as a transient species. For all these reasons, we consider that the safest option in astrochemical models is to explicitly include $HCNH_2$. This is the approach that we are taking in future works.

Once the proton transfer reaction is discussed, we can focus on the reactions with atomic hydrogen. The reaction 26 is the only reaction investigated in this work that is barrierless in the doublet spin channel. The chemical rationale for this finding is that being a singlet carbene, $HCNH_2$ is extremely reactive in the carbon center. The associated reaction energy is consequentially also the highest among all reactions that occur in the doublet channel, of $\Delta U^{R,26}_{Ice}$ = -268.8 kJ mol^{-1} ($\Delta U^{R,26}_{Gas}$ = -298.5 kJ mol^{-1}), which is a value closer to those found for radical-radical reactions, especially in the case of the gas-phase reaction.

The DFT results are supported by our own multireference calculations (See Supplementary Information). Therefore we exclude aminomethylene from being a stable node in the reaction network.

Contrary to what happens in reaction 26, the other hydrogenation reaction (reaction 27) presents a very high activation energy, $\Delta U_{Ice}^{\ddagger,27}$ = 101.9 kJ mol^{-1}. Interestingly, this reaction in the gas phase presents a moderately lower activation energy, $\Delta U_{Gas}^{\ddagger,27}$ = 73.8 kJ mol^{-1}. Due to the geometry of the TS, reaction 27 in ice requires breaking hydrogen bonds in addition to the intrinsic barrier. We find a similar gap in the reaction energies, again associated with the strength of the hydrogen bonds in the reactant and product, $\Delta U_{Ice}^{R,27}$ = -55.5 kJ mol^{-1} and $\Delta U_{Gas}^{R,27}$ = -26.9 kJ mol^{-1}. Overall, the importance of this reaction in the entire reaction scheme simulated here must be negligible.

The study of the reactivity of $HCNH_2$ concludes with the abstraction reactions 28 and 29. Beginning with the reaction 28 on the H_2O ice, we find a small barrier of $\Delta U_{Ice}^{\ddagger,28}$ = 3.5 kJ mol^{-1}. In the gas phase, this barrier is $\Delta U_{Gas}^{\ddagger,28}$ = 5.8 kJ mol^{-1}. The reaction energy is also slightly different between ice and gas for the reaction 28, i.e. $\Delta U_{Ice}^{R,28}$ = -109.3 kJ mol^{-1} *vs* $\Delta U_{Gas}^{R,28}$ = -91.1 kJ mol^{-1}.

Finally, for the reaction 29, we also found a different behavior between ice and gas. However, for this particular reaction, barriers emerge in both cases with activation energies $\Delta U_{Ice}^{\ddagger,29}$ = 22.7 kJ mol^{-1} and $\Delta U_{Gas}^{\ddagger,29}$ = 29.4 kJ mol^{-1} and reaction energies $\Delta U_{Ice}^{R,29}$ = -171.2 kJ mol^{-1} and $\Delta U_{Gas}^{R,29}$ = -163.2 kJ mol^{-1}. The viability of the reaction 29 must be measured against the alternative reactions discussed in the preceding paragraphs. Because this reaction competes with barrierless and low barrier channels (Reactions 26–28), we consider it to be not relevant in the chemistry of H_xCNH_y molecules.

Summarizing, the hydrogenation of HNC can either lead to a H-mediated isomerization to HCN or evolve to more complex molecules through $HCNH_2$ or H_2CNH; the latter is a rather stable node in the reaction network. Further hydrogenation of these species leads, among other products, to H_2CNH_2 and H_3CNH. While chemistry of H_2CNH_2 was discussed in Section 3.2.2, H_3CNH, can be easily hydrogenated to H_3CNH_2 through:

$$^2H_3CNH + {}^2H \longrightarrow {}^1H_3CNH_2, \qquad (30)$$

which is an alternative way to form H_3CNH_2. For the sake of completeness we consider alternative reaction branches,

$$^2H_3CNH + {}^2H \longrightarrow {}^1H_2CNH + H_2 \qquad (31)$$
$$^2H_3CNH + {}^2H \longrightarrow {}^3H_3CN + H_2. \qquad (32)$$

From this set of reactions, reaction 31 is studied at the B level of theory while reaction 32 is studied at the A level, because it occurs in the triplet state (see below).

Reaction 30 is barrierless in both ice and gas with $\Delta U_{Ice}^{R,30}$ = -403.3 kJ mol^{-1} ($\Delta U_{Gas}^{R,30}$ = -400.3 kJ mol^{-1}), which is one of the highest reaction energies in the present work. This is due to the formation of the totally saturated and stable H_3CNH_2 molecule. The abstraction reactions 31 and 32 were studied in different spin channels because hydrogenation reactions were studied in the most stable channel. For H_2CNH this is clearly the singlet one, but H_3CN is revealed to be stable in the triplet channel. Reaction 31 has a small activation energy on ice and gas of $\Delta U_{Ice}^{\ddagger,31}$ = 1.8 kJ mol^{-1} and $\Delta U_{Gas}^{\ddagger,31}$ = 1.3 kJ mol^{-1}. Such barriers are minute and easily overcome by quantum tunneling. The reaction energy for reaction 31 is $\Delta U_{Ice}^{R,31}$ = -288.2 kJ mol^{-1} ($\Delta U_{Gas}^{R,31}$ = -281.3 kJ mol^{-1}). Finally, reaction 32 also has an activation barrier of $\Delta U_{Ice}^{\ddagger,32}$ = 12.9 kJ mol^{-1} ($\Delta U_{Gas}^{\ddagger,32}$ = 8.8 kJ mol^{-1}) and a lower reaction energy than the other reactions studied for this species, $\Delta U_{Ice}^{R,32}$ = -76.3 kJ mol^{-1} ($\Delta U_{Gas}^{R,32}$ = -85.8 kJ mol^{-1}). Because reaction 32 takes place in the triplet channel it does not compete with reactions 30 or 31.

3.2.6 Hydrogenation of HCN

In Section 3.2.5 we showed how HCN can be formed from HNC. The reactivity of HCN is different to the one of HNC, because reaction

$$^1HCN + {}^2H \longrightarrow {}^2HCNH, \qquad (33)$$

has activation energies of $\Delta U_{Ice}^{\ddagger,33}$ = 37.3 kJ mol^{-1} ($\Delta U_{Gas}^{\ddagger,33}$ = 41.3 kJ mol^{-1}) and reaction energies of $\Delta U_{Ice}^{R,33}$ = -43.0 kJ mol^{-1} ($\Delta U_{Gas}^{R,33}$ = -52.1 kJ

mol^{-1}).

Alternatively, addition of H to HCN in the HC moiety towards H_2CN:

$$^1\mathrm{HCN} + {}^2\mathrm{H} \longrightarrow {}^2\mathrm{H_2CN}. \quad (34)$$

Reaction 34 shows an activation energy and reaction energy on ice of $\Delta U_{\mathrm{Ice}}^{\ddagger,34}$ = 20.1 kJ mol^{-1} and $\Delta U_{\mathrm{Ice}}^{R,34}$ = -110.0 kJ mol^{-1}. The values in the gas phase are slightly different, $\Delta U_{\mathrm{Gas}}^{\ddagger,34}$ = 25.4 kJ mol^{-1} and $\Delta U_{\mathrm{Gas}}^{R,34}$ = -108.5 kJ mol^{-1}, indicating a stabilization of the transition state on the surface. On ice, the activation energy is significant, therefore confirmation of its viability with calculations including nuclear quantum effects (e.g. including quantum tunneling) is required.

The product of the reaction, H_2CN (methylene amidogen), is a radical that has gained recent attention, along with the CNH_2 radical discussed previously, due to the fact that the abundance ratio between the two in the gas-phase can serve as a possible temperature tracer of interstellar environments.[70,71] The interaction of H_2CN with H on dust grains can take place through the following three reactions:

$$^2\mathrm{H_2CN} + {}^2\mathrm{H} \longrightarrow {}^3\mathrm{H_3CN} \quad (35)$$
$$^2\mathrm{H_2CN} + {}^2\mathrm{H} \longrightarrow {}^1\mathrm{H_2CNH} \quad (36)$$
$$^2\mathrm{H_2CN} + {}^2\mathrm{H} \longrightarrow {}^1\mathrm{HCN} + {}^1\mathrm{H_2}. \quad (37)$$

Of these reactions, both reactions 36 and 37 are studied with the B level of theory as it corresponds to open-shell singlet radical-radical couplings, while reaction 35 is studied at the A level of theory, because it proceeds in the triplet channel (H_3CN is a triplet in the ground state). All proton transfer reactions are endothermic, because H_2CN is the global minimum of the H_xC-NH_y; $x + y = 2$ system.

The addition reaction 35 has an activation barrier that we estimate in $\Delta U_{\mathrm{Ice}}^{\ddagger,35}$ = 9.0 kJ mol^{-1} ($\Delta U_{\mathrm{Gas}}^{\ddagger,35}$ = 11.1 kJ mol^{-1}) and a reaction energy of $\Delta U_{\mathrm{Ice}}^{R,35}$ = -140.6 kJ mol^{-1} ($\Delta U_{\mathrm{Gas}}^{R,35}$ = -142.7 kJ mol^{-1}). We also found a barrier in the reaction 36, but in this case it is so small that it submerges after the correction for ZPVE. This submerged barrier is totally absent in the gas-phase, even for electronic energies, showing that it is a barrier ineherent to the H_2O matrix (see above and Enrique-Romero et al.[13] for an in-depth discussion of such barriers appearing in radical recombination in ices). The reaction energy for reaction 36 is $\Delta U_{\mathrm{Ice}}^{R,36}$ = -357.5 kJ mol^{-1} ($\Delta U_{\mathrm{Gas}}^{R,36}$ = -350.9 kJ mol^{-1}).

In the case of the abstraction reaction 37, we again observe the presence of small electronic energy barriers that are present both in the gas and in the ice, and that submerge after inclusion of ZPVE. Submerged barriers are only below -1.9 and -0.6 kJ mol^{-1} for ice and gas, respectively. The values of these barriers are below the sensitivity of the B level of theory. Nevertheless, if the reaction would have a barrier, it would be small and easily to overcome by quantum tunneling. Finally, the reaction energies of reaction 37 are $\Delta U_{\mathrm{Ice}}^{R,37}$ = -291.3 kJ mol^{-1} ($\Delta U_{\mathrm{Gas}}^{R,37}$ = -296.2 kJ mol^{-1}).

Among the reactions studied for this species we see that addition to H_2CNH (reaction 36) and the abstraction back to HCN (reaction 37) are the most likely pathways, although addition to C in the triplet channel (reaction 35) has a moderately low barrier and proceeds in a different PES, meaning that there is no competition for the reaction. In general, H_2CN has been revealed to be a transient radical that forms closed shell molecules such as HCN or H_3CNH_2. It is also a good example of a transient species detectable in the ISM.[70,71]

After reaction 36, further hydrogenations on H_2CNH proceed as explained in Section 3.2.5. When the product of the reaction is HCN (Reaction 37), the subsequent reactions are the ones considered in this section. Finally, H_3CN, formed through reaction 35, can be hydrogenated as:

$$^3\mathrm{H_3CN} + {}^2\mathrm{H} \longrightarrow {}^2\mathrm{H_3CNH} \quad (38)$$
$$^3\mathrm{H_3CN} + {}^2\mathrm{H} \longrightarrow {}^2\mathrm{H_2CN} + {}^1\mathrm{H_2}. \quad (39)$$

These reactions are investigated at the B level of theory. Reaction 38 is barrierless with a reaction energy of $\Delta U_{\mathrm{Ice}}^{R,38}$ = -346.8 kJ mol^{-1} ($\Delta U_{\mathrm{Gas}}^{R,38}$ = -335.7 kJ mol^{-1}). The reaction 39 is not intrinsically barrierless, since it sports a barrier in electronic energy. Such a barrier vanishes upon inclusion of ZPVE in the ice model, but remains in the gas model. However, the activation energy for the gas is very low ($\Delta U_{\mathrm{Gas}}^{\ddagger,39}$ = 0.5 kJ mol^{-1}). The reaction energies for the ice and gas models are

very similar, $\Delta U_{Ice}^{R,39}$ = -269.9 kJ mol^{-1} ($\Delta U_{Gas}^{R,39}$ = -264.6 kJ mol^{-1}). The small barriers or lack thereof for H_3CN indicate that H_3CN must be a transient species in the reaction network and in the chemistry of the ISM. Finally, we also looked for possible proton transfer mechanisms starting from H_3CN, finding endothermic and thus nonviable paths.

As in the case of HCN, if H_3CN is reverted back *via* a hydrogen abstraction reaction, it reforms H_2CN, resulting in a net zero sum after two reactions with hydrogen. On the other hand, when reaction 38 takes place, it forms H_3CNH, that, as we showed in Section 3.2.5, most likely forms H_3CNH_2, the endpoint of our network, *via* reaction 30

4 Discussion

A summary of the reaction energies and activation energies in the ice phase and in the gas phase, when applicable, is provided in Tables 1 and 2. These tables, along with Figure 2 serve as the basis for the text.

The relative stability of $^3CNH_3$ to unimolecular processes (i.e. proton transfer reactions and triple-singlet decay), combined with its high reactivity for hydrogenation, makes the reaction network that we study in this work particularly complicated. The reaction network is characterized by four nodes, which are closed-shell molecules whose further reactivity requires a surmount or tunneling through kinetic barriers. These nodes are HNC, HCN, H_2CNH, and H_3CNH_2. Among them, H_3CNH_2 shows the highest activation energies for its destruction (Section 3.2.3). Besides, the activation energies required to hydrogenate HNC are relatively low. Similar arguments can be given for H_2CNH and HCN, although these molecules are significantly more resilient to hydrogenation than HNC. Therefore, we conclude that in the steady state, such as the conditions found in hydrogenation experiments with high H fluxes, the abundance of H_3CNH_2 must dominate.[75]

It is also important to note that the route to H_3CNH_2 can be experimentally tractable by isotopic substitution. Because the routes directly connecting $CNH_3 \xrightarrow{D} HD_2CNH_2/D_3CNH_2$ are barrierless, the addition of deuterium would also be facile, in contrast to deuteration starting from HCN. The latter has at least two steps with a barrier and consequentially a reduced quantum tunneling efficiency. Moreover, starting from HCN necessarily requires reactions at the N center, unlike in the case starting from CNH_3. For instance, N-D infrared bands could be used to trace the dominant reaction pathway.

We note that HCN/HNC partake in many other reaction networks apart from the one studied here, including gas phase synthesis, which increases their abundances. In astronomical environments, recent observations and chemical modeling of H_3CNH_2 toward different cold and hot cores support that HCN hydrogenation must be an important source of H_3CNH_2.[76] Although this rationalization is useful to visualize the most abundant final product of the network, it is also simplistic because under ISM conditions there is an interplay between gas and grain processes; e.g gas phase synthesis[77,78] feeds molecules onto icy dust. We also note that the H accretion rate (e.g. H fluxes) on interstellar dust are lower under ISM conditions than in experiments. Astrochemical rate equation models are fundamental to contextualize atomistic data to interstellar environments. The expansion of widely used reaction networks with the reaction schemes presented here and other recent work[15,19,27] is in our immediate plans.

Another discussion pertaining to astrophysical environments concerns how the chemical network presented here can modify isomeric ratios, and most significantly the H_2CN/CNH_2 ratio recently discussed in the literature.[30,70] At low temperatures and in the gas phase, this ratio is close to 1.0 due to the dominance of gas chemistry, which does not produce a preferential isomer.[30,70,71,77] This is similar to the well studied HCN/HNC ratio that depends markedly on gas temperature,[79] due to preferential destruction reactions in the gas, e.g $HNC + H \longrightarrow HCN + H$. The dependence of H_2CN/CNH_2 on temperature is not yet well understood. In cold environments, both isomers should form without particular preference, and the H_2CN/CNH_2 ratio is close to one in the Taurus Molecular Cloud (TMC-1).[30] However, at the center of our galaxy, in G+0.693-0.027, this ratio in-

creases. In this work, we show that the conversion of HCN to H_2CN through reaction 34 proceeds with a moderate activation energy. On the contrary, the conversion of HNC to CNH_2 (Reaction 15) has a very high activation energy and therefore is not a suitable formation pathway. Because both HCN and HNC are stable nodes in our reaction network, we hypothesize that a higher hydrogenation of HCN may lead to an excess of H_2CN in grains, which is later reflected in observations after desorption by a non-thermal mechanism such as shock-induced desorption, characteristic of G+0.693-0.027. Although this preferential increase of the H_2CN/CNH_2 may be behind the observations,[70] definitive confirmation requires dedicated astrochemical modeling, including gas phase reactions.

An interesting conundrum derived from our calculations is the comparison with the previous work of Talbi and Ellinger[80], where the activation energies of reactions 33 and 16 were found to be significantly different from those presented here, of 74.5 and 17.6 kJ mol^{-1}, respectively. We believe that the reason behind the disagreement is that the authors of Talbi and Ellinger[80] considered that both reactions 33 and 16 led to trans-HCNH, rather than cis-HCNH. We confirmed that the correct product of the hydrogenation must be cis-HCNH by performing IRC calculations from the TS in the gas phase for both reactions. Therefore, we may explain the disagreement based on this argument, where in Talbi and Ellinger[80] some torsion energy may be added to the transition state. More difficult to explain is the disagreement with reaction HCN + H $\longrightarrow$ H_2CN (reaction 34, discussed above), where Talbi and Ellinger[80] found an activation energy of 63.6 kJ mol^{-1}. This high barrier is in contradiction with the experiments shown in Theule et al.[75] where sequential hydrogenation of HCN ice reportedly yields H_3CNH_2, something that would be impossible considering the low temperatures of the experiment (15 K) and the high hydrogenation barriers predicted in Talbi and Ellinger[80]. Our new calculations align better with the experiments of Theule et al.[75] We also note that our calculations agree very well with those shown in Majumdar et al.[81], which report gas-phase activation energies of 28.3 kJ mol^{-1} for reaction 34, for example, 2.9 kJ mol^{-1} lower than our own values (25.4 kJ mol^{-1}), strengthening the accuracy of our results.

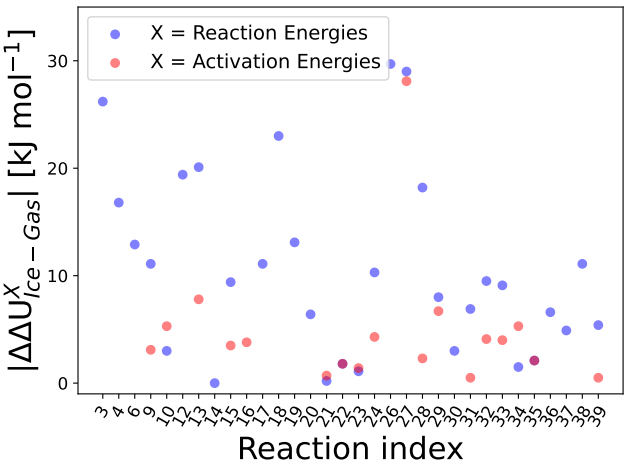

Figure 5: Energy differences ($\Delta\Delta U^x_{\text{Ice - Gas}}$ for the reaction energies (blue dots) and activation energies (red dots) for the reactions studied in this work using a gas phase model and a $(H_2O)_{14}$ cluster model. Omitted reactions include proton transfers, that are exclusive of the cluster model, and reactions that we deem not relevant on the cluster model (See text).

From a chemical perspective, it is interesting to evaluate the differences in the chemistry that arise from the reactions on ice and in the gas. Unsigned differences for the relevant reactions are plotted in Figure 5. As expected, we observe a higher variability in the reaction energies (ΔU^R) compared to the activation energies ($\Delta U^\ddagger$). This is due to the difference in the binding of the product and reactant to the surface, i.e., the change in binding energies. For the transition state, the binding energy is close to that of the reactants and therefore the change in $\Delta U^\ddagger$ is less pronounced. The only exception in $\Delta U^\ddagger$ is found for the reaction 27, because on ice this reaction involves the addition of an H to the -NH_2 moiety and the break of the associated H bond. The same explanation also holds for the second reaction with the highest difference in $\Delta U^\ddagger$ between ice and gas, reaction 13. In general, we find that for hydrogenations and H abstraction reactions, $\Delta U^\ddagger$ does not increase or decrease dramatically on the surface, and a gas phase model is suitable in many cases. A gas-phase model can be useful to determine intrinsic activation energies in complex cases, e.g. the three reactions 6–8 in this study, for which the TS on the cluster model were difficult to determine.

From the point of view of astrochemical models, the most important magnitude is $\Delta U^{\ddagger}$, with ΔU^{R} being important in the study of chemical desorption (See below).[82] The similarity in $\Delta U^{\ddagger}$ between the gas-phase values and cluster is also helpful in determining the impact of using a single water cluster in our study, a necessity imposed by the computational constraints associated with the large number of chemical reactions considered. As we said in Section 2, using a single cluster is a caveat of our simulations, because not only different dilutions can be present in different astronomical sources (for example, between 3–10 % in Young Stellar Objects , YSO), according to Boogert et al.[44], but also several binding sites are possible for NH_3 and C adsorption. The limited variability between gas-phase and cluster values in our calculated quantities, which represent an extreme case in the description of the reaction matrix, indicates also a small variability for binding sites and dilutions. We note that this is not generally the case, depending on each system under consideration. Finally, we also note that proton transfer reaction do depend on the local environment, and a study similar to Baiano et al.[63] or Perrero et al.[26] for key proton transfer reaction (i.e. neither barrierless nor having a high barrier) like reaction 25 can be helpful to predict barriers.

Atomic carbon condensation has recently been proven to be an alternative source to explain the surge of COMs in cold interstellar environments.[14,15,17–20,83] Briefly summarizing the results in the literature, Potapov et al.[16] and Molpeceres et al.[15] showed that carbon atoms associate without a barrier with ASW. A fraction of them remain chemisorbed,[15] others react further with H_2O to form formaldehyde (H_2CO) through reactions mediated by proton shuttles,[16,27,84] and finally some others remain physisorbed and can diffuse to chemisorption sites or react with molecules.[20] On CO ices, the accretion of C atoms forms the CCO radical that upon hydrogenation forms ketene (H_2CCO),[17,19] that can further react eventually forming acetaldehyde (CH_3CHO).[19] Because there is no H-bonding network on CO ices, CCO requires the action of H atoms to react, unlike the case of ASW. Recently, Krasnokutski et al.[18] performed codeposition experiments of CO:NH_3:C finding the formation of aminoketene (NH_2HCCO) and its spontaneous polymerization. In between the cases of H_2O and CO we find NH_3, which is a major component of the interstellar dust surface, with a relative abundance to water of 3–10%,[44] Using a cluster model that mimicks such composition ($\sim$ 1/14), we observed that $^3CNH_3$ is formed without a barrier through reaction 1, and that it is more resilient than COH_2 on the ASW ice matrix, something coherent with the experiments of Krasnokutski et al.[18] on CO (apolar matrix). The resilience of CNH_3 compared to COH_2 is important, because the formation of H_2CO is irreversible and acts as the beginning of the formation of oxygen-bearing COMs. In this work, we found that C accretion on NH_3 and subsequent hydrogenation is an efficient way of forming N-bearing COMS. ForCNH_3, the formation of COMs and their precursors, for example methylamine (H_3CNH_2) and methanimine (H_2CNH) compete with hydrogenation through H-abstraction reactions to HNC/HCN, reducing the budget of N-bearing COMs. However, our results also show that HCN and HNC can be hydrogenated under high H fluxes, in agreement with the literature.[75]

Finally, we dedicate some words to the possibility of the return of the synthesized grain molecules to the gas phase of the ISM, where they can be detected using radiotelescopes. One of the postulated mechanisms for the return of molecules to the gas at shallow temperatures is chemical desorption, i.e. the use of the reaction energy to promote desorption before thermalization of the nascent molecule. Several studies have already addressed the topic of chemical desorption on interstellar grains,[85–88] all pointing to the reaction energy ΔU^{R}, the number of vibrational degrees of freedom of the formed molecule, and the binding energy as crucial factors for its occurrence. The radical coupling reactions in this study are promising candidates for efficient chemical desorption, due to the large ΔU^{R}. However, this factor must be weighed against the other two factors mentioned above. A meticulous study of binding energy distributions of the moleculesof this reaction network can shed some light on the viability of chemical desorption for the reactions studied here. It is also important to highlight that chemical desorption depends on dynamic aspects such as energy redistribution to the surface or other internal

molecular modes,[87,89–92] which are less straightforward to determine for each species. Overall, from the point of view of chemical models, in absence of a specific study on energy transfer for the molecule, we suggest to continue using the available analytic expressions in the literature,[85–87] that in all cases constitute an advantage over the use of constant desorption probabilities.

5 Conclusions

Using quantum chemical calculations, we studied the $H_xC\text{-}NH_y$ hydrogenation reaction network starting from the $^3CNH_3$ chemisorbate that is formed barrierlessly on a water cluster including an ammonia molecule. Because $^3CNH_3$ is stable, it can stay long enough on the surface to react with H atoms, opening a new way to synthesize N-bearing COMs. The hydrogenation reaction network is shown to be rather complex and hints at a competition between the formation of methylamine, a relatively abundant N-bearing COM,[76] and the formation of simpler triatomic acids (HCN / HNC). However, hydrogenation of HCN / HNC is easier than abstraction of H in methylamine, which supports the notion that methylamine must be the end point of the reaction network. Our results also help to rationalize the formation of aminoketene from $CO + NH_3 + C$ in recent experiments,[18] by ensuring that CNH_3 should survive in the surface long enough to experience reactivity in the absence of H atoms and in apolar environments. Finally, the reaction network studied here provides data to be incorporated into astrochemical models, which can be used in combination with recent efforts in the literature to unravel the importance of carbon-driven chemistry.[16,17,19,20,27,84] A study of the impact of carbon chemistry on the formation, evolution, and segregation of COMs will be presented in a subsequent work using astrochemical rate equation models. Finally, we remark that deepening into the description of quantum tunneling for borderline reactions in our reaction network remains a crucial step to discard some of the reactions with moderate activation energies.

Acknowledgement G.M. thanks the Japan Society for the Promotion of Science, JSPS International Fellow P22013, and the Grant-in-aid JP22F22013 for its support. G.M also acknowledges support from the grant RYC2022-035442-I funded by MCIN/AEI/10.13039/501100011033 and FSE+. The authors acknowledge the support of the state of Baden-Württemberg through bwHPC and the German Research Foundation (DFG) through grant no INST 40/575-1 FUGG (JUSTUS 2 cluster) and the Research Center for Computational Science, Okazaki, Japan (Projects: 22-IMS-C301, 23-IMS-C128). KF acknowledges support from JSPS KAKENHI grant numbers 20H05847 and 21K13967. Y.A. acknowledges support from Grant-in-Aid for Scientific Research (S) 18H05222 and Grant-in-Aid for Transformative Research Areas (A) grant Nos. 20H05847. MT acknowledges support from JSPS KAKENHI grant numbers JP23H03982 and JP21H01139. V.M.R. and D.S.A. acknowledge the funds provided by the Consejo Superior de Investigaciones Científicas (CSIC) and the Centro de Astrobiología (CAB) through the project 20225AT015 (Proyectos intramurales especiales del CSIC). V.M.R. has also received support from the grant number RYC2020-029387-I funded by MICIU/AEI/10.13039/501100011033 and by "ESF, Investing in your future". D.S.A. also extends his gratitude for the financial support provided by the Comunidad de Madrid through the Grant PIPF-2022/TEC-25475. V.M.R and L.C. acknowledges financial support from the grant No. PID2022-136814NB-I00 by the Spanish Ministry of Science, Innovation and Universities/State Agency of Research MICIU/AEI/10.13039/501100011033 and by "ERDF A way of making Europe". L.C also acknowledges additional funding of the MICIU/AEI through grant PID2019-105552RB-C41.

Supporting Information Available

The electronic supporting information includes: Multireference check of barrierless nature of certain hydrogen abstraction / addition reactions. Expansion of the discussion for the $HCNH_3 \longrightarrow H_2CNH_2$ reaction. Structures of the TS found in this work for the reactions on the ice.

References

(1) Herbst, E.; Van Dishoeck, E. F. Complex organic interstellar molecules. *Annual Review*

of Astronomy and Astrophysics **2009**, *47*, 427–480, Publisher: Annual Reviews ISBN: 0066-4146.

(2) Watanabe, N.; Kouchi, A. Efficient Formation of Formaldehyde and Methanol by the Addition of Hydrogen Atoms to CO in H_2O-CO Ice at 10 K. *The Astrophysical Journal* **2002**, *571*, L173–L176, Publisher: IOP Publishing.

(3) Fuchs, G. W.; Cuppen, H. M.; Ioppolo, S.; Romanzin, C.; Bisschop, S. E.; Andersson, S.; Van Dishoeck, E. F.; Linnartz, H. Hydrogenation Reactions in Interstellar CO Ice Analogues. *Astronomy and Astrophysics* **2009**, *505*, 629–639.

(4) Garrod, R. T. A Three-phase Chemical Model of Hot Cores: The Formation of Glycine. *The Astrophysical Journal* **2013**, *765*, 60.

(5) Garrod, R. T.; Jin, M.; Matis, K. A.; Jones, D.; Willis, E. R.; Herbst, E. Formation of Complex Organic Molecules in Hot Molecular Cores through Nondiffusive Grain-surface and Ice-mantle Chemistry. *The Astrophysical Journal Supplement Series* **2022**, *259*, 1.

(6) Balucani, N.; Ceccarelli, C.; Taquet, V. Formation of complex organic molecules in cold objects: the role of gas-phase reactions. *Monthly Notices of the Royal Astronomical Society: Letters* **2015**, *449*, L16–L20.

(7) Vazart, F.; Latouche, C.; Skouteris, D.; Balucani, N.; Barone, V. CYANOMETHANIMINE ISOMERS in COLD INTERSTELLAR CLOUDS: INSIGHTS from ELECTRONIC STRUCTURE and KINETIC CALCULATIONS. *Astrophys. J.* **2015**, *810*, 111.

(8) Cooke, I. R.; Sims, I. R. Experimental Studies of Gas-Phase Reactivity in Relation to Complex Organic Molecules in Star-Forming Regions. *ACS Earth and Space Chemistry* **2019**, *3*, 1109–1134, Publisher: American Chemical Society.

(9) Redondo, P.; Barrientos, C.; Largo, A. Complex Organic Molecules Formation in Space Through Gas Phase Reactions: A Theoretical Approach. *The Astrophysical Journal* **2017**, *836*, 240.

(10) Barone, V.; Puzzarini, C. Toward Accurate Formation Routes of Complex Organic Molecules in the Interstellar Medium: The Paradigmatic Cases of Acrylonitrile and Cyanomethanimine. *Frontiers in Astronomy and Space Sciences* **2022**, *8*, 814384.

(11) Jin, M.; Garrod, R. T. Formation of Complex Organic Molecules in Cold Interstellar Environments through Nondiffusive Grain-surface and Ice-mantle Chemistry. *The Astrophysical Journal Supplement Series* **2020**, *249*, 26.

(12) Enrique-Romero, J.; Ceccarelli, C.; Rimola, A.; Skouteris, D.; Balucani, N.; Ugliengo, P. Theoretical computations on the efficiency of acetaldehyde formation on interstellar icy grains. *Astronomy & Astrophysics* **2021**, *655*, A9.

(13) Enrique-Romero, J.; Rimola, A.; Ceccarelli, C.; Ugliengo, P.; Balucani, N.; Skouteris, D. Quantum Mechanical Simulations of the Radical–Radical Chemistry on Icy Surfaces. *The Astrophysical Journal Supplement Series* **2022**, *259*, 39.

(14) Ruaud, M.; Loison, J. C.; Hickson, K. M.; Gratier, P.; Hersant, F.; Wakelam, V. Modelling complex organic molecules in dense regions: Eley-Rideal and complex induced reaction. *Monthly Notices of the Royal Astronomical Society* **2015**, *447*, 4004–4017.

(15) Molpeceres, G.; Kästner, J.; Fedoseev, G.; Qasim, D.; Schömig, R.; Linnartz, H.; Lamberts, T. Carbon Atom Reactivity with Amorphous Solid Water: H_2O-Catalyzed Formation of H_2CO. *Journal of Physical Chemistry Letters* **2021**, *12*, 10854–10860, Publisher: American Chemical Society.

(16) Potapov, A.; Jäger, C.; Henning, T. Ice Coverage of Dust Grains in Cold Astrophysical

Environments. *Physical Review Letters* **2020**, *124*, 221103.

(17) Fedoseev, G.; Qasim, D.; Chuang, K.-J.; Ioppolo, S.; Lamberts, T.; van Dishoeck, E. F.; Linnartz, H. Hydrogenation of Accreting C Atoms and CO Molecules-Simulating Ketene and Acetaldehyde Formation Under Dark and Translucent Cloud Conditions. *The Astrophysical Journal* **2022**, *924*, 110.

(18) Krasnokutski, S. A.; Chuang, K.-J.; Jäger, C.; Ueberschaar, N.; Henning, T. A pathway to peptides in space through the condensation of atomic carbon. *Nature Astronomy* **2022**, *6*, 381–386.

(19) Ferrero, S.; Ceccarelli, C.; Ugliengo, P.; Sodupe, M.; Rimola, A. Formation of Complex Organic Molecules on Interstellar CO Ices? Insights from Computational Chemistry Simulations. *The Astrophysical Journal* **2023**, *951*, 150.

(20) Tsuge, M.; Molpeceres, G.; Aikawa, Y.; Watanabe, N. Surface diffusion of carbon atoms as a driver of interstellar organic chemistry. *Nature Astronomy* **2023**, *7*, 1351–1358.

(21) Tielens, A. G. G. M. *The Physics and Chemistry of the Interstellar Medium*, 1st ed.; Cambridge University Press, 2005.

(22) Wakelam, V.; Loison, J. C.; Mereau, R.; Ruaud, M. Binding energies: New values and impact on the efficiency of chemical desorption. *Molecular Astrophysics* **2017**, *6*, 22–35.

(23) Rimola, A.; Skouteris, D.; Balucani, N.; Ceccarelli, C.; Enrique-Romero, J.; Taquet, V.; Ugliengo, P. Can Formamide Be Formed on Interstellar Ice? An Atomistic Perspective. *ACS Earth and Space Chemistry* **2018**, *2*, 720–734.

(24) Shimonishi, T.; Nakatani, N.; Furuya, K.; Hama, T. Adsorption Energies of Carbon, Nitrogen, and Oxygen Atoms on the Low-temperature Amorphous Water Ice: A Systematic Estimation from Quantum Chemistry Calculations. *The Astrophysical Journal* **2018**, *855*, 27.

(25) Duflot, D.; Toubin, C.; Monnerville, M. Theoretical Determination of Binding Energies of Small Molecules on Interstellar Ice Surfaces. *Frontiers in Astronomy and Space Sciences* **2021**, *8*, 24.

(26) Perrero, J.; Enrique-Romero, J.; Martínez-Bachs, B.; Ceccarelli, C.; Balucani, N.; Ugliengo, P.; Rimola, A. Non-energetic Formation of Ethanol via CCH Reaction with Interstellar H2O Ices. A Computational Chemistry Study. *ACS Earth and Space Chemistry* **2022**, *6*, 496–511, Publisher: American Chemical Society.

(27) Ferrero, S.; Ceccarelli, C.; Ugliengo, P.; Sodupe, M.; Rimola, A. Formation of Interstellar Complex Organic Molecules on Water-rich Ices Triggered by Atomic Carbon Freezing. *The Astrophysical Journal* **2024**, *960*, 22.

(28) Eley, D. D.; Rideal, E. K. Parahydrogen conversion on tungsten [5]. *Nature* **1940**, *146*, 401–402, Publisher: Nature Publishing Group ISBN: 0028-0836.

(29) Bourgalais, J.; Capron, M.; Abhinavam Kailasanathan, R. K.; Osborn, D. L.; Hickson, K. M.; Loison, J.-C.; Wakelam, V.; Goulay, F.; Le Picard, S. D. The $C(^3P) + NH_3$ Reaction in Interstellar Chemistry. I. Investigation of the Product Formation Channels. *The Astrophysical Journal* **2015**, *812*, 106.

(30) Agúndez, M.; Roncero, O.; Marcelino, N.; Cabezas, C.; Tercero, B.; Cernicharo, J. The chemistry of H_2NC in the interstellar medium and the role of the $C + NH_3$ reaction. *Astronomy & Astrophysics* **2023**, *673*, A24.

(31) Minissale, M.; Congiu, E.; Baouche, S.; Chaabouni, H.; Moudens, A.; Dulieu, F.; Accolla, M.; Cazaux, S.; Manicó, G.; Pirronello, V. Quantum tunneling of oxygen atoms on very cold surfaces. *Physical Review Letters* **2013**, *111*, 053201.

(32) Lee, M. W.; Meuwly, M. Diffusion of atomic oxygen relevant to water formation in amorphous interstellar ices. *Faraday Discuss.* **2014**, *168*, 205–222, Publisher: The Royal Society of Chemistry.

(33) Minissale, M.; Congiu, E.; Dulieu, F. Direct measurement of desorption and diffusion energies of O and N atoms physisorbed on amorphous surfaces. *Astronomy and Astrophysics* **2016**, *585*, A146.

(34) Zaverkin, V.; Molpeceres, G.; Kästner, J. Neural-network assisted study of nitrogen atom dynamics on amorphous solid water – II. Diffusion. *Monthly Notices of the Royal Astronomical Society* **2022**, *510*, 3063–3070.

(35) Tielens, W., A.G.G.M and Hagen Model calculations of the molecular composition of interstellar grain mantles. *Astronomy and Astrophysics* **1982**, *114*, 245–260.

(36) Oba, Y.; Watanabe, N.; Hama, T.; Kuwahata, K.; Hidaka, H.; Kouchi, A. WATER FORMATION THROUGH A QUANTUM TUNNELING SURFACE REACTION, OH + H $_2$, AT 10 K. *The Astrophysical Journal* **2012**, *749*, 67.

(37) Meisner, J.; Lamberts, T.; Kästner, J. Atom Tunneling in the Water Formation Reaction $H_2 + OH \rightarrow H_2O + H$ on an Ice Surface. *ACS Earth and Space Chemistry* **2017**, *1*, 399–410.

(38) Goldsmith, P. F.; Li, D. H I Narrow Self-Absorption in Dark Clouds: Correlations with Molecular Gas and Implications for Cloud Evolution and Star Formation. *Astrophysical Journal* **2005**, *622*, 938–958.

(39) Molpeceres, G.; García de la Concepción, J.; Jiménez-Serra, I. Diastereoselective Formation of Trans-HC(O)SH through Hydrogenation of OCS on Interstellar Dust Grains. *The Astrophysical Journal* **2021**, *923*, 159.

(40) Álvarez Barcia, S.; Russ, P.; Kästner, J.; Lamberts, T. Hydrogen transfer reactions of interstellar complex organic molecules. *Monthly Notices of the Royal Astronomical Society* **2018**, *479*, 2007–2015.

(41) Markmeyer, M. N.; Lamberts, T.; Meisner, J.; Kästner, J. HOCO formation in astrochemical environments by radical-induced H-abstraction from formic acid. *Monthly Notices of the Royal Astronomical Society* **2019**, *482*, 293–300.

(42) Molpeceres, G.,; Jiménez-Serra, I.,; Oba, Y.,; Nguyen, T.,; Watanabe, N.,; de la Concepción, J. García,; Maté, B.,; Oliveira, R.,; Kästner, J., Hydrogen abstraction reactions in formic and thioformic acid isomers by hydrogen and deuterium atoms. *A&A* **2022**, *663*, A41.

(43) Molpeceres, G.; Rivilla, V. M.; Furuya, K.; Kästner, J.; Maté, B.; Aikawa, Y. Processing of hydroxylamine, NH_2OH, an important prebiotic precursor, on interstellar ices. *Monthly Notices of the Royal Astronomical Society* **2023**, *521*, 6061–6074.

(44) Boogert, A. C.; Gerakines, P. A.; Whittet, D. C. Observations of the icy universe. *Annual Review of Astronomy and Astrophysics* **2015**, *53*, 541–581.

(45) Tinacci, L.; Germain, A.; Pantaleone, S.; Ferrero, S.; Ceccarelli, C.; Ugliengo, P. Theoretical Distribution of the Ammonia Binding Energy at Interstellar Icy Grains: A New Computational Framework. *ACS Earth and Space Chemistry* **2022**, *6*, 1514–1526.

(46) Zhao, Y.; Truhlar, D. G. Hybrid meta density functional theory methods for thermochemistry, thermochemical kinetics, and noncovalent interactions: The MPW1B95 and MPWB1K models and comparative assessments for hydrogen bonding and van der Waals interactions. *Journal of Physical Chemistry A* **2004**, *108*, 6908–6918, Publisher: American Chemical Society.

(47) Zhao, Y.; Truhlar, D. G. Design of density functionals that are broadly accurate for thermochemistry, thermochemical kinetics, and nonbonded interactions. *J. Phys. Chem. A* **2005**, *109*, 5656–67.

(48) Grimme, S.; Antony, J.; Ehrlich, S.; Krieg, H. A consistent and accurate ab initio parametrization of density functional dispersion correction (DFT-D) for the 94 elements H-Pu. *Journal of Chemical Physics* **2010**, *132*, 154104.

(49) Grimme, S.; Ehrlich, S.; Goerigk, L. Effect of the damping function in dispersion corrected density functional theory. *Journal of Computational Chemistry* **2011**, *32*, 1456–1465, Publisher: John Wiley & Sons, Ltd.

(50) Weigend, F.; Ahlrichs, R. Balanced basis sets of split valence, triple zeta valence and quadruple zeta valence quality for H to Rn: Design and assessment of accuracy. *Physical Chemistry Chemical Physics* **2005**, *7*, 3297–3305.

(51) Zheng, J.; Xu, X.; Truhlar, D. G. Minimally augmented Karlsruhe basis sets. *Theoretical Chemistry Accounts* **2011**, *128*, 295–305.

(52) Goerigk, L.; Hansen, A.; Bauer, C.; Ehrlich, S.; Najibi, A.; Grimme, S. A look at the density functional theory zoo with the advanced GMTKN55 database for general main group thermochemistry, kinetics and noncovalent interactions. *Physical Chemistry Chemical Physics* **2017**, *19*, 32184–32215, Publisher: The Royal Society of Chemistry.

(53) Metz, S.; Kästner, J.; Sokol, A. A.; Keal, T. W.; Sherwood, P. ChemShell-a modular software package for QM/MM simulations. *Wiley Interdisciplinary Reviews: Computational Molecular Science* **2014**, *4*, 101–110.

(54) Kästner, J.; Carr, J. M.; Keal, T. W.; Thiel, W.; Wander, A.; Sherwood, P. DL-FIND: An open-source geometry optimizer for atomistic simulations*. *Journal of Physical Chemistry A* **2009**, *113*, 11856–11865, Publisher: American Chemical Society ISBN: 1520-5215 (Electronic)\r1089-5639 (Linking).

(55) Riplinger, C.; Pinski, P.; Becker, U.; Valeev, E. F.; Neese, F. Sparse maps—A systematic infrastructure for reduced-scaling electronic structure methods. II. Linear scaling domain based pair natural orbital coupled cluster theory. *The Journal of Chemical Physics* **2016**, *144*, 024109.

(56) Guo, Y.; Riplinger, C.; Becker, U.; Liakos, D. G.; Minenkov, Y.; Cavallo, L.; Neese, F. Communication: An improved linear scaling perturbative triples correction for the domain based local pair-natural orbital based singles and doubles coupled cluster method [DLPNO-CCSD(T)]. *The Journal of Chemical Physics* **2018**, *148*, 011101.

(57) Papajak, E.; Zheng, J.; Xu, X.; Leverentz, H. R.; Truhlar, D. G. Perspectives on Basis Sets Beautiful: Seasonal Plantings of Diffuse Basis Functions. *Journal of Chemical Theory and Computation* **2011**, *7*, 3027–3034.

(58) Neese, F. The ORCA program system. *WIREs Computational Molecular Science* **2012**, *2*, 73–78, Publisher: John Wiley & Sons, Ltd.

(59) Neese, F.; Wennmohs, F.; Becker, U.; Riplinger, C. The ORCA quantum chemistry program package. *Journal of Chemical Physics* **2020**, *152*, 224108.

(60) Neese, F. Software update: The ORCA program system–Version 5.0. *WIREs Computational Molecular Science* **2022**, *12*, e1606.

(61) Cuppen, H. M.; Karssemeijer, L. J.; Lamberts, T. The kinetic Monte Carlo method as a way to solve the master equation for interstellar grain chemistry. *Chemical Reviews* **2013**, *113*, 8840–8871.

(62) Sameera, W. M. C.; Jayaweera, A. P.; Ishibashi, A.; Hidaka, H.; Oba, Y.; Watanabe, N. A systematic mechanistic survey on the reactions between OH radical and CH3OH on ice. *Faraday Discuss.* **2023**, *245*, 508–518.

(63) Baiano, C.; Lupi, J.; Barone, V.; Tasinato, N. Gliding on Ice in Search of Accurate and Cost-Effective Computational Methods for

Astrochemistry on Grains: The Puzzling Case of the HCN Isomerization. *Journal of Chemical Theory and Computation* **2022**, *18*, 3111–3121.

(64) Papakondylis, A.; Mavridis, A. Electronic Structure and Bonding of the Fastidious Species CN_2 and CP_2 : A First-Principles Study. *The Journal of Physical Chemistry A* **2019**, *123*, 10290–10302.

(65) Joshi, P. R.; Lee, Y.-P. A chemical link between methylamine and methylene imine and implications for interstellar glycine formation. *Communications Chemistry* **2022**, *5*, 62.

(66) Henkelman, G.; Uberuaga, B. P.; Jónsson, H. A climbing image nudged elastic band method for finding saddle points and minimum energy paths. *The Journal of Chemical Physics* **2000**, *113*, 9901–9904.

(67) Kerkeni, B.; Clary, D. C. Quantum scattering study of the abstraction reactions of H atoms from CH3NH2. *Chemical Physics Letters* **2007**, *438*, 1–7.

(68) Oba, Y.; Chigai, T.; Osamura, Y.; Watanabe, N.; Kouchi, A. Hydrogen isotopic substitution of solid methylamine through atomic surface reactions at low temperatures: A potential contribution to the D/H ratio of methylamine in molecular clouds. *Meteoritics & Planetary Science* **2014**, *49*, 117–132.

(69) Henkelman, G.; Jónsson, H. A dimer method for finding saddle points on high dimensional potential surfaces using only first derivatives. *The Journal of Chemical Physics* **1999**, *111*, 7010–7022.

(70) San Andrés, D.; Colzi, L.; Rivilla, V. M.; García de la Concepción, J.; Melosso, M.; Martín-Pintado, J.; Jiménez-Serra, I.; Zeng, S.; Martín, S.; Requena-Torres, M. A. H2CN/H2NC abundance ratio: a new potential temperature tracer for the interstellar medium. *Monthly Notices of the Royal Astronomical Society* **2023**, *523*, 3239–3250.

(71) Cabezas, C.; Agúndez, M.; Marcelino, N.; Tercero, B.; Cuadrado, S.; Cernicharo, J. Interstellar detection of the simplest aminocarbyne H_2NC: an ignored but abundant molecule. *Astronomy & Astrophysics* **2021**, *654*, A45.

(72) Wakelam, V.; Bron, E.; Cazaux, S.; Dulieu, F.; Gry, C.; Guillard, P.; Habart, E.; Hornekær, L.; Morisset, S.; Nyman, G.; Pirronello, V.; Price, S. D.; Valdivia, V.; Vidali, G.; Watanabe, N. H_2 formation on interstellar dust grains: The viewpoints of theory, experiments, models and observations. *Molecular Astrophysics* **2017**, *9*, 1–36.

(73) Godfrey, P. D.; Brown, R. D.; Robinson, B. J.; Sinclair, M. W. Discovery of Interstellar Methanimine (Formaldimine). *Astrophys. Lett.* **1973**, *13*, 119.

(74) Eckhardt, A. K.; Schreiner, P. R. Spectroscopic Evidence for Aminomethylene (H-C-NH_2)-The Simplest Amino Carbene. *Angewandte Chemie International Edition* **2018**, *57*, 5248–5252.

(75) Theule, P.; Borget, F.; Mispelaer, F.; Danger, G.; Duvernay, F.; Guillemin, J. C.; Chiavassa, T. Hydrogenation of solid hydrogen cyanide HCN and methanimine CH_2NH at low temperature. *Astronomy & Astrophysics* **2011**, *534*, A64.

(76) Suzuki, T.; Majumdar, L.; Goldsmith, P. F.; Tokuda, K.; Minamoto, H.; Ohishi, M.; Saito, M.; Hirota, T.; Nomura, H.; Oya, Y. Survey of CH_3NH_2 and its Formation Process. *The Astrophysical Journal* **2023**, *954*, 189.

(77) Loison, J.-C.; Wakelam, V.; Hickson, K. M. The interstellar gas-phase chemistry of HCN and HNC. *Monthly Notices of the Royal Astronomical Society* **2014**, *443*, 398–410.

(78) Yang, Z.; Medvedkov, I. A.; Goettl, S. J.; Kaiser, R. I. Low-Temperature Gas-Phase Formation of Methanimine (CH_2NH; X^1A') the Simplest Imine under Single-Collision Conditions. *The Journal of Physical Chemistry Letters* **2023**, 8500–8506.

(79) Hacar, A.; Bosman, A. D.; Van Dishoeck, E. F. HCN-to-HNC intensity ratio: a new chemical thermometer for the molecular ISM. *Astronomy & Astrophysics* **2020**, *635*, A4.

(80) Talbi, D.; Ellinger, Y. Isomerization versus hydrogen exchange reaction in the HNC ¡=¿ HCN conversion. *Chemical Physics Letters* **1996**, *263*, 385–392.

(81) Majumdar, L.; Loison, J.-C.; Ruaud, M.; Gratier, P.; Wakelam, V.; Coutens, A. Methyl isocyanate (CH_3NCO): an important missing organic in current astrochemical networks. *Monthly Notices of the Royal Astronomical Society: Letters* **2018**, *473*, L59–L63.

(82) Cuppen, H. M.; Walsh, C.; Lamberts, T.; Semenov, D.; Garrod, R. T.; Penteado, E. M.; Ioppolo, S. Grain Surface Models and Data for Astrochemistry. *Space Science Reviews* **2017**, *212*, 1–58.

(83) Potapov, A.; Bouwman, J.; Jäger, C.; Henning, T. Dust/ice mixing in cold regions and solid-state water in the diffuse interstellar medium. *Nature Astronomy* **2021**, *5*, 78–85.

(84) Molpeceres, G.; Kästner, J. Computational Study of the Hydrogenation Sequence of the Phosphorous Atom on Interstellar Dust Grains. *The Astrophysical Journal* **2021**, *910*, 55.

(85) Garrod, R. T.; Wakelam, V.; Herbst, E. Non-thermal desorption from interstellar dust grains via exothermic surface reactions. *Astronomy & Astrophysics* **2007**, *467*, 1103–1115.

(86) Minissale, M.; Dulieu, F.; Cazaux, S.; Hocuk, S. Dust as interstellar catalyst I. Quantifying the chemical desorption process. *Astronomy & Astrophysics* **2015**, *585*, A24.

(87) Fredon, A.; Cuppen, H. M. Molecular dynamics simulations of energy dissipation and non-thermal diffusion on amorphous solid water. *Physical Chemistry Chemical Physics* **2018**, *20*, 5569–5577, Publisher: The Royal Society of Chemistry.

(88) Fredon, A.; Groenenboom, G. C.; Cuppen, H. M. Molecular Dynamics Simulations of Energy Dissipation on Amorphous Solid Water: Testing the Validity of Equipartition. *ACS Earth and Space Chemistry* **2021**, *5*, 2032–2041.

(89) Pantaleone, S.; Enrique-Romero, J.; Ceccarelli, C.; Ugliengo, P.; Balucani, N.; Rimola, A. Chemical desorption versus energy dissipation: insights from ab-initio molecular dynamics of HCO formation. *The Astrophysical Journal* **2020**, *897*, 56.

(90) Pantaleone, S.; Enrique-Romero, J.; Ceccarelli, C.; Ferrero, S.; Balucani, N.; Rimola, A.; Ugliengo, P. H 2 Formation on Interstellar Grains and the Fate of Reaction Energy. *The Astrophysical Journal* **2021**, *917*, 49, Publisher: American Astronomical Society.

(91) Ferrero, S.; Pantaleone, S.; Ceccarelli, C.; Ugliengo, P.; Sodupe, M.; Rimola, A. Where Does the Energy Go during the Interstellar NH_3 Formation on Water Ice? A Computational Study. *The Astrophysical Journal* **2023**, *944*, 142.

(92) Molpeceres, G.; Zaverkin, V.; Furuya, K.; Aikawa, Y.; Kästner, J. Reaction dynamics on amorphous solid water surfaces using interatomic machine-learned potentials: Microscopic energy partition revealed from the P + H $\rightarrow$ PH reaction. *Astronomy & Astrophysics* **2023**, *673*, A51.

Graphical TOC Entry